Ultrahigh-pressure transitions in solid hydrogen

Ho-kwang Mao and Russell J. Hemley

Geophysical Laboratory and Center for High Pressure Research,
Carnegie Institution of Washington, Washington, D.C. 20015

During the past five years, major progress has been made in the experimental study of solid hydrogen at ultrahigh pressures as a result of developments in diamond-cell technology. Pressures at which metallization has been predicted to occur have been reached (250–300 Gigapascals). Detailed studies of the dynamic, structural, and electronic properties of dense hydrogen reveal a system unexpectedly rich in physical phenomena, exhibiting a variety of transitions at ultrahigh pressures. This colloquium explores the study of dense hydrogen as an archetypal problem in condensed-matter physics.

CONTENTS

I. INTRODUCTION

The use of pressure as a means of altering the physical and chemical states of materials is as fundamental as varying temperature or chemical composition. As a result of experimental limitations, however, the impact of high-pressure studies on the development of condensed-matter science has been comparatively small. These limitations have now been surmounted by recent breakthroughs in the area of diamond-cell technology. The diamond cell is an instrument small enough to fit in the palm of your hand, yet powerful enough to reach static pressures an order of magnitude higher than those attainable by previous techniques. It is now possible to generate multimegabar pressures [a megabar is approximately one million atmospheres, or 100 Gigapascals (GPa) in SI units]. Perhaps even more significant than the enormous pressure range now accessible is the fact that the diamonds are excellent windows through which the sample can be viewed. Better yet, we can also use a wide range of electromagnetic radiation to characterize the physical properties of samples *in situ* at high pressures. These newly acquired capabilities enable us to explore fully the effects of the pressure variable. Indeed, in the small number of systems investigated to date, observation of unexpected behavior in materials at ultrahigh pressures has been the rule rather than the exception.

The search for such phenomena logically begins with hydrogen, the "simplest" element, the first entry in the Periodic Table, and by far the most abundant element in the solar system. At low pressures, hydrogen crystallizes as an insulating molecular solid, but it was recognized in the early years of quantum mechanics that at extreme pressure conditions hydrogen would form a dense plasma (Fowler, 1926). At high compression electrons would no longer remain stable localized in bonds or in core states and would instead delocalize, an idea leading to Bernal's conjecture that at sufficiently high pressures all materials will become metallic (see Wigner and Huntington, 1935). In their classic study, Wigner and Huntington (1935) were the first to predict that, under extreme pressure, the molecules of solid hydrogen will dissociate to form a monatomic metallic solid (Fig. 1), and this was predicted to occur at pressures of 25 GPa. Theoretical calculations carried out over the next sixty years have given rise to the expectation that such a dense metallic solid, in either an atomic or a molecular metallic state, could possess a number of unusual, if not exotic, properties (Ashcroft, 1968; Brovman *et al.*, 1972). Its study at high pressure has been described as a key problem in modern physics and astrophysics (Ginzburg, 1978). As a result, the creation of "metallic hydrogen" in the laboratory has become one of the principal goals of high-pressure research.

During the past several years, a great deal of progress has been made in the experimental study of solid hydrogen at ultrahigh pressures. Static pressures above 250 GPa have now been applied to the material. This pres-

sure far exceeds not only Wigner and Huntington's origi-nal estimate of the molecular dissociation pressure, but also many recent calculations of the molecular hydrogen metallization pressure. A variety of surprising new phe-nomena have been observed by *in situ* spectroscopic stud-ies. For example, an intriguing phase transition was ob-served near 150 GPa in both hydrogen and deuterium (Hemley and Mao, 1988, 1989; Lorenzana et al., 1989). Unique features of this transition include a large low-temperature discontinuity in the frequency of the molec-ular vibron (Hemley and Mao, 1988, 1989; Lorenzana et al., 1989), a large increase in infrared absorption and reflectivity (Mao et al., 1990; Hanfland et al., 1993), and a triple point on its P-T phase line. A new view emerges from recent experimental and theoretical studies that, despite its putative "simplicity," the behavior of hydro-gen at very high densities is more interesting, unusual, and rich in physical phenomena than previously thought.

The need for accurate measurements of the properties of hydrogen has led to the advancement of ultrahigh-pressure technology in general. Studies of hydrogen marked the first confinement of condensed gases above 250 GPa (Hemley and Mao, 1988, 1989), the first micro-Raman measurement above 60 GPa (Sharma et al., 1980a) and 200 GPa (Hemley and Mao, 1988), the first infrared measurements above 50 GPa (Mao et al., 1984) and 200 GPa (Hanfland et al., 1993), the first single-crystal x-ray diffraction above 20 GPa (Mao et al., 1988), the first neutron diffraction above 30 GPa (Glazkov et al., 1988), the first Brillouin scattering measurement above 20 GPa (Shimizu et al., 1981), and the first appli-cation of synchrotron infrared spectroscopy at megabar pressures (Hanfland et al., 1992). These developments have been essential for testing hypotheses and exploring unpredicted high-pressure behavior of hydrogen, includ-ing physical phenomena perhaps unique to the conditions of extreme pressure.

II. SOLID HYDROGEN AS AN ARCHETYPAL SYSTEM

At low pressures and temperatures, hydrogen is a di-atomic molecular solid with strong covalent molecular bonds, weak intermolecular interactions, and a filled valence band with a large band gap, which makes the ma-terial a good insulator.[1] After a half century of work, the properties of the low-pressure solid are generally well es-tablished [see Silvera (1980) and van Kranendonk (1983) for reviews]. Solid hydrogen is the archetypal quantum solid and formally the only quantum molecular solid. The solid is characterized by molecules in free (or nearly free) rotational states, strong quantum behavior of its nu-clei, and large intermolecular (lattice vibration) anhar-monicity. Due to the nearly spherical charge distribution of the molecules, it behaves in many ways like a rare-gas solid.[2]

At low densities, symmetry considerations, regarding the nuclear spin (I) and rotational states (J) of the mole-cules, give rise to the para- (p) and ortho- (o) hydrogen designation for the even and odd J species, respectively. For deuterium, ortho designates the even J, and para the odd J species.[3] The equilibrium concentration of odd:even J species is zero at $T=0$ K, increasing with temperature to 3:1 for hydrogen and to 1:2 for deuterium at room temperature (Silvera, 1980), and designated nor-mal (n) hydrogen or deuterium, respectively. Differences in ortho and para concentrations can have a large effect on properties at zero pressure. Owing to electric quadrupole-quadrupole (EQQ) interactions,[4] for example, pure $J=1$ o-H_2 and p-D_2 (described by nonspherical wave functions) transform to a structure with long-range orientational order below 3–4 K. Strictly speaking, the ortho-para designation is only applicable to hydrogen where J is a good quantum number and the crystal's wave function can be represented as a product of molecu-

---

[1] The bond length in the solid at ambient pressure is essentially unchanged from that of the free molecule ($R=0.74$ Å) with a much larger intermolecular distance (3.8 Å). The dissociation energy D_e for the free molecules is 4.48 eV and 4.56 eV, and the ionization energy is 15.43 eV and 15.47 eV, for H_2 and D_2, re-spectively (Huber and Herzberg, 1979). For the solid the valence-conduction band gap is near 16 eV, with optical excita-tions (excitons) beginning at 11 eV (see Hemley et al., 1991).

[2] As a result, the intermolecular potential is largely isotropic at low pressures; that is, $\phi(r,\theta,\phi) \approx \phi(r)$, where r is the distance between molecular centers and θ and ϕ describe the relative orientation of the molecular bond (or axis of quantization of the rotational wave functions).

[3] This difference arises from the difference in nuclear spins I. In hydrogen, $I=\frac{1}{2}$ and the nuclei are bosons, whereas in deu-terium $I=1$ and the nuclei are fermions [see van Kranendonk (1983)].

[4] The electric quadrupole (EQ) moment is given by $Q^{20}=Q^{(2)}Y_{20}(\theta,\phi)$, where $Y_{20}(\theta,\phi)$ is the spherical harmonic. This is the leading-order anisotropic interaction in the solid at low densities.
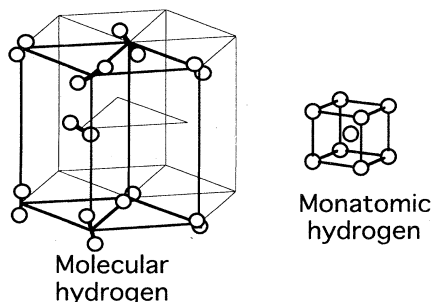

Monatomic
hydrogen

Molecular
hydrogen

FIG. 1. Idealized structures of solid molecular hydrogen (disor-dered hexagonal-close packed) and of atomic metallic hydrogen (body-centered-cubic structure, bcc). Wigner and Huntington (1935) assumed the bcc structure for the high-pressure phase but indicated that similar results are expected for any Bravais lattice.

lar rotational wave functions, as is the case at low densities.

The application of high pressure brings the hydrogen molecules closer together in the crystal lattice. Consequently, interactions between molecules increase. At some critical density, the solid will attain a lower free energy and a higher density if the molecules dissociate. This monatomic phase of hydrogen must be a metal if it has an odd number of atoms Z per primitive unit cell [such as the monatomic bcc phase ($Z = 1$) studied by Wigner and Huntington (1935)] and hence a half-filled band.[5] At very high pressures, hydrogen could thus resemble a monatomic alkali metal. In contrast to the alkali metals, however, a hydrogen atom has only one electron, so that all electrons would be delocalized to form an electron gas, leaving only protons at the lattice sites. In fact, its properties could differ considerably from those of the alkali metals: as an extremely light metal with strong quantum motion of the nuclei and no core electron, atomic hydrogen may possess many exotic properties, including high-temperature superconductivity (Ashcroft, 1968) and a liquidlike metallic ground state (Brovman et al., 1972).[6]

We thus have a fascinating system with two boundary conditions representing diametrically opposed types of solids—a low-pressure molecular insulator and a high-pressure free-electron atomic metal. Moreover, we now know experimentally that between these two extremes hydrogen undergoes a series of intermediate transitions, some gradual, some abrupt. As shown below, some very interesting physics manifests itself at the boundaries between these phases. Theoretical studies carried out in the mid 1970s indicated that metallization might occur in the molecular phase, producing molecular metallic hydrogen via band overlap before reaching the monatomic metal (Ramaker et al., 1975; Friedli and Ashcroft, 1977).[7] Further calculations have predicted that the molecular metal could also exhibit unusual properties (e.g., Moulopoulos and Ashcroft, 1991; Ashcroft, 1993). The unique features of hydrogen—including quantum solid behavior, coupling of its molecular angular momentum

and nuclear spin, competition between free rotation and orientational order, and possible destabilization of the molecular (paired) state at high densities—thus compound the complexity (or enrich the physics!) of its high-pressure behavior.

The following questions have been posed regarding the vast range of compression between hydrogen's molecular insulator and metallic states—at least a factor of ten in density. What are the crystal structures of various high-pressure polymorphic phases of molecular and atomic solids? At what pressure and temperature will the molecules orientationally order, and what is the nature of the ordering? Is the ordering transition gradual or sudden? How does the molecular orientation, and hence the full symmetry of crystalline hydrogen, affect its physical, chemical, and electronic properties? Does the energy of the valence-conduction band gap decrease with pressure, and if so, will the gap close completely to form a molecular metal before molecular dissociation? If band-overlap metallization occurs, will it be isostructural? Could such a transition exhibit the behavior originally envisaged by Mott with a discontinuity at low temperature, a continuous transition at high temperature, and a P-T critical point? Is there evidence for destabilization of the paired (molecular state), and if so, what does this imply for the magnitude of the electron-phonon (molecular vibration) coupling? What is the effect of the large zero-point motion of the nuclei when molecules are brought closer at high density? Could the large zero-point motion force dense hydrogen into a quantum fluid at low temperature?

The previously inaccessible compressional space of hydrogen provides a fertile field in which to examine these questions. Some answers are already emerging, but they have led to more questions as studies progress. By analogy to the contribution of low-pressure hydrogen studies to the development of modern physics and quantum chemistry, the study of this "simple" system may shed new light on the physics of condensed matter at very high densities.

III. HIGH-PRESSURE DIAMOND-CELL TECHNIQUES

Pressure is the crucial variable underlying this vast new area of study. With the diamond cell as a vehicle, it has become possible in the past five years to perform static experiments under calibrated pressures above 300 GPa. Not only has the pressure range been greatly extended, but the arsenal of techniques used to probe materials under these conditions has also been expanded and improved.

Static pressures in the megabar range were first attained in 1976 using the Mao-Bell diamond-anvil cell (Mao and Bell, 1976, 1978), which, along with its subsequent variations, has become the primary tool of multimegabar static pressure research (Jayaraman, 1983; Mao, 1989). A schematic drawing of a diamond-anvil cell is shown in Fig. 2. Since pressure is simply force divided by area, enormous pressures can be generated by

---

[5]The possibility of the dissociated phase's having an even number of atoms per cell has arisen in recent theoretical studies of new classes of structures, including the prediction that monatomic hydrogen is stable in a diamond structure ($Z = 2$) (Natoli et al., 1993).

[6]Even more exotic possibilities have been proposed for the nonmolecular phase. For hydrogen a quantum liquid ground state implies a two-component Fermi liquid, which in turn could possess superconductivity (Oliva and Ashcroft, 1981). Moreover, because the deuterium nucleus is a boson, it has been suggested that it might exhibit both superconductivity and superfluidity (see Oliva and Ashcroft, 1981)!

[7]This might occur in a manner akin to molecular iodine (Balchan and Drickamer, 1961). In this mechanism, the energy of the valence-conduction band gap decreases with increasing pressure and eventually vanishes (the point band-gap closure).
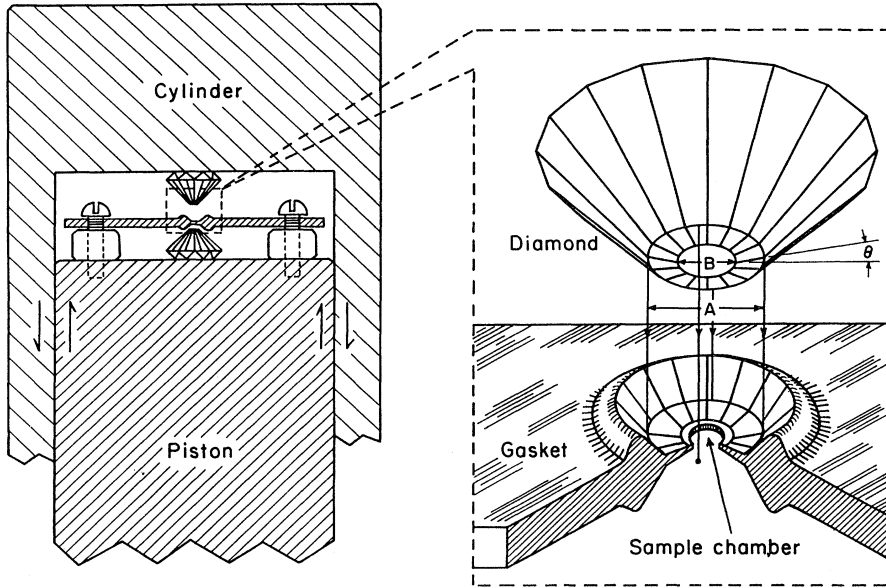
FIG. 2. Schematic drawing of a megabar diamond-anvil cell. Critical design parameters for use of the cell to multimegabar pressures is the diameter of the central flat B of the diamond culet and the bevel angle θ. Design features are discussed in Mao and Bell (1976, 1978) and Mao (1989).

anvils with a very small tip ($B = 20$ to 600 μm in diameter), as long as the anvil material is strong enough to withstand pressure without yielding. Flawless single-crystal diamonds are chosen for making anvils, since diamonds are the strongest material known to man. The anvils exert pressure on a thin metallic gasket within which a circular sample chamber is confined. When pressure exceeds the yield strength of the gasket material (3 to 5 GPa), the ductile flow of the gasket transmits pressure to the sample. The flow stops when the gasket becomes sufficiently thin (2 to 60 μm) and reaches mechanical equilibrium via a gradient of pressures, thus forming a passive supporting ring for the sample chamber.

Diamonds are transparent to radiation from a wide range of the electromagnetic spectrum—including high-energy x and γ radiation above 10 keV (wavelengths shorter than 1.25 Å) and lower-energy ultraviolet-visible-infrared radiation below 5 eV (wavelengths longer than 250 nm). As a result, numerous diffraction, scattering, and absorption probes can be employed for investigating the electronic, molecular, and crystallographic structure of samples under pressure. An important constraint on diamond-cell technology is the limited anvil size (~ 0.3–0.4 carat, 1 ct. $= 0.2$ g). Large, flawless, single-crystal diamonds are rare and prohibitively expensive, since the diamond price increases quadratically with increasing size.[8] Given a constant anvil size, there is a tradeoff between maximum pressure and maximum sample volume (Mao, 1989). For instance, at 50 GPa, the sample can be as large as a nanoliter; in the multimegabar range, it is subpicoliter. Therefore the maximum

pressures possible for a given type of measurement depend upon the sample-size requirement of the particular analytical technique.

Great progress in microsample spectroscopic techniques has been made via recent advances on two fronts—the development of powerful radiation sources and improved detection systems (Mao, 1989; Hanfland et al., 1992). Lasers and synchrotrons provide collimated beams of electromagnetic radiation many orders of magnitude more brilliant than that available from conventional light sources. Multichannel detector technologies—energy dispersive x-ray detectors, storage-phosphorous x-ray imaging plates, intensified diode array detectors, charge-coupled detectors, and Fourier-transform infrared interferometers—effectively allow parallel detection of a band of wavelengths, thereby improving measurement sensitivity for the study of ultrasmall samples at ultrahigh pressures.

IV. HYDROGEN AT HIGH DENSITIES— AN EXPERIMENTAL OVERVIEW

A. Confining hydrogen under pressure

While multimegabar pressures had been achieved consistently with other materials, the study of hydrogen at ultrahigh pressures presented many experimental challenges. Two handicaps had to be overcome: (1) hydrogen is a difficult sample to contain physically and chemically, and (2) many of hydrogen's high-pressure properties are difficult to measure. Low-density gaseous hydrogen had to be densified considerably (by up to a factor of ~ 1000) before being introduced into the diamond cell. For instance, because it is a small and reactive atom, hydrogen tends to embrittle and fracture materials it encounters; it also tends to react to form hydrides with just about all gasket metals. A proper gasket material had to be developed with sufficient strength to withstand ul-

---

[8]The largest diamond ever used as an anvil was 4 ct. (Glazkov et al., 1988) and had a market value of over $100,000. In contrast, a typical 0.4 ct. diamond costs $\sim \$1,000$.

trahigh pressure, while at the same time remaining ductile and resisting embrittlement by hydrogen. Flawless diamond anvils were selected to avoid the premature fracturing caused by hydrogen.

In 1978, Mao and Bell successfully loaded hydrogen in a diamond cell by cooling the cell to 15 K and condensing gaseous hydrogen to a liquid in the open sample chamber (Mao and Bell, 1979). The diamond anvils were then driven together to seal the chamber. The fluid hydrogen sample trapped in the gasket hole was warmed to room temperature (295 K) and pressurized to 5.4 GPa to form a clear, colorless, crystalline solid. This hydrogen crystal was then pressurized to ~50 GPa and found to remain transparent. Numerous subsequent experiments utilized low-temperature loading or a room-temperature, high-pressure gas-filling technique pioneered by Mills et al. (1980). Developments in diamond-cell technology over the next 15 years gradually led to studies of hydrogen at pressures beyond 200 GPa.

B. High-pressure probes

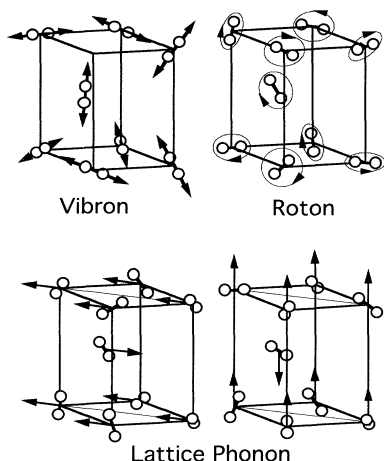The crystal structure is one of the most fundamental pieces of information needed for characterizing a materi-

Vibron   Roton

Lattice Phonon

FIG. 3. Principal vibrational excitations in solid hydrogen ($k=0$). The pure molecular vibration excitation (vibron) is designated $Q_{\Delta v}(J)$, where v is the vibrational quantum number, Δ the difference between the final and the initial levels, and J the rotational quantum number. Letters O,P,Q,R,S, denote $\Delta J = -2, -1, 0, 1, 2$, respectively. For example, $Q_1(0)$ signifies one quantum of excitation of the vibron with $J=0$ and $\Delta J=0$ (4161 cm^{-1} and 2993 cm^{-1} for H_2 and D_2, respectively, in the gas phase). Likewise, $Q_2(0)$ denotes an excitation of the vibron with two quanta (vibron overtone, or bivibron) at close to twice the frequency. The rotational spectrum for the free molecule is given by the $BJ(J+1)$, where B is the rotational constant (59.31 cm^{-1} and 29.91 cm^{-1} for free H_2 and D_2, respectively); in the solid crystal field effects lift the degeneracy of the rotational levels. For example, $S_0(J)$ represents pure roton excitations ($\Delta J=2$); i.e., $S_0(0)$ for $J=0$, $S_0(1)$ for $J=1$, etc. The lattice phonons include the degenerate E_{2g} (transverse-optic, or TO) mode, which is Raman-active, and the B_{2g} (longitudinal-optic, or LO) mode. In addition to overtones, combination excitations involving different modes can be measured [e.g., $Q_1(1)+S_0(1)$].

al at high pressure. Theoretical studies, for example, usually begin with explicit knowledge of the crystal structure, and the pressure (and temperature dependence) of structure properties provides crucial thermodynamic information through the equation of state (volume or density as a function of pressure). Diffraction, the basic technique for determination of crystal structures and equations of state, was thought to be impracticable for use with solid hydrogen above a few GPa. X-ray diffraction intensity is proportional to the squared atomic number. H_2, with an atomic number of one, is an extremely weak x-ray scatterer. The problem was eventually solved by utilizing synchrotron radiation and energy dispersive x-ray diffraction techniques (Mao et al., 1988). Neutron diffraction can also be used, but so far only for D_2 because of its higher scattering cross section (Glazkov et al., 1988). The elasticity of hydrogen can be determined by Brillouin spectroscopy (Shimizu et al., 1981). The maximum pressures for the study of hydrogen with these techniques is currently limited to ~50 GPa, although this limit is rising steadily with technical improvements.[9]

At higher pressures, various optical spectroscopies are the primary techniques for probing the dense solid, including both its vibrational and electronic excitations. The principal vibrational excitations of hydrogen are shown and described in Fig. 3: These are the intramolecular stretches (vibrons), rotations (rotons), and lattice vibrations (phonons), where the name of the collective excitation in the solid is given in parentheses. Raman spectroscopy, which measures shifts of these excitations relative to the laser frequency, has been particularly important for hydrogen studies because it can be used to study small samples with a spatial resolution close to the diffraction limit of visible light (~1 μm). Recently, infrared vibrational spectroscopy has become an especially powerful technique with the development and application of synchrotron radiation methods. Infrared dipole absorption is forbidden in the free hydrogen molecule but

---

[9]A number of other techniques can be used in this lower pressure range but have not yet been extended to megabar pressures, including both magnetic and electric methods (e.g., Mao and Bell, 1981; Lee et al., 1989). In particular, direct electrical conductivity techniques have been developed for studies of metallization and electronic transport at lower pressures (Mao and Bell, 1981). These techniques employ electrical leads which are insulated from one another and from the metal gasket. The configuration of the circuit and insulation must be maintained with the leads in contact with the sample without breaking or shorting during deformation of the assembly by the pressure of the anvil. Such measurements become increasingly difficult above 100 GPa and are currently unreliable with very small samples, although this direction merits active pursuit, especially with microcircuitry technology. Far more information about electronic properties has been obtained so far by noncontact measurements with spectroscopic probes, as described below.

becomes allowed as a result of intermolecular interactions and is highly sensitive to density. Hence, measurements of IR vibrational spectra can reveal detailed information about intermolecular interactions in the high-density solid. Optical absorption and reflection spectroscopy in the near ultraviolet to the infrared can be used to probe electronic transitions. At lower densities the energies of such excitations are above the absorption threshold of the diamond anvils (5.4 eV) and are therefore not directly accessible by conventional spectroscopic techniques.[10] However, information can be obtained from measurements in the visible range, and these excitation energies shift to lower values with pressure, as described below.

C. Experimental tests

Studies of hydrogen at ultrahigh pressures have been typically carried out in previously uncharted territory. Newly developed techniques must be tested for possible unexpected physical and chemical effects. Control experiments testing the validity of a measurement are as essential as the measurement itself. Therefore, for reporting new results, we have adhered to the following guidelines, performing approximately 45 separate experiments on hydrogen above 100 GPa:

(1) Perform direct experiments at high pressure. The history of the field has demonstrated the pitfalls of long extrapolation; indeed, extrapolation tends to miss the underlying physics. (2) Reproduce the results multiple times. Experimental difficulties restrict this guideline from general practice in ultrahigh-pressure studies of other materials. (3) Vary the P-T conditions. (4) Study hydrogen isotopes (H_2, D_2, HD). The large isotopic mass ratio provides an important test of a number of properties, as well as a control. To first order, the isotopes are similar in electronic properties, scale with mass in vibrational properties, and are different in rotational, ordering, and phonon coupling properties. Conformity or deviation from this pattern can provide additional insight for interpreting new observations. (5) Test for unusual behavior and contamination by varying the type of diamond (IA, IB, IIA, or IIB), gasket material, presence of ruby pressure calibrant, etc. (6) Run control experiments with samples other than hydrogen (e.g., Ne, NaCl, SiO_2, etc.). (7) Confirm the presence of molecular hydrogen by

observing the vibron.[11]

The emerging picture of hydrogen at high density is discussed in the following sections. We focus on ultrahigh-pressure transitions in the solid, which can involve changes in crystallographic, orientational, and electronic structure, either independently or jointly. In the interest of clarity and consistency, we adopt the convention of designating polymorphic phases with Roman numerals, using this nomenclature without specific structural implications.

V. PHASE I—THE QUANTUM MOLECULAR SOLID

Phase I spans a large P-T range, from zero pressure to approximately 150 GPa, within which the density of solid hydrogen increases ninefold. As a result, the physical properties of the solid evolve extensively, exhibiting extraordinary changes in some cases. The solid remains an insulator in this phase.

A. Crystal structure and elasticity

Abrikosov (1954) proposed a high-pressure crystal structure for the molecular solid and calculated the compressibility (equation of state), and pointed out the importance of these properties for understanding higher-pressure behavior including metallization.[12] In subsequent years, estimates of structural and thermodynamic properties differed widely because of a lack of sufficiently accurate techniques—both experimentally and theoretically—to study the molecular phase at high pressure. In 1988, the first single-crystal diffraction measurements were performed on H_2 and D_2 (Glazkov et al., 1988; Mao et al., 1988), providing the first accurate studies of the structure and equation of state at very high pressures (>6 GPa). There is now good agreement among various equation-of-state determinations to the

---

[10]This is the intrinsic absorption edge for diamond at ambient pressure (Type IIa diamonds). The threshold is lower for commonly used Type I anvils (~ 3 eV) due to nitrogen impurities. These absorptions shift into the visible spectrum above 200 GPa (see, for example, Mao and Hemley, 1991).

---

[11]This list covers common, or predictable, experimental problems. For example, Ruoff and Vanderborgh (1991) claimed to show that hydrogen chemically reduced the ruby pressure calibrant to form metallic aluminum at 136 GPa and further postulated that the reflectance measurement of hydrogen at 177 GPa by Mao et al. (1990) was actually that of aluminum. However, control experiments on the hydrogen-ruby system had in fact been performed (see Mao et al., 1992). In addition, the claim of hydrogen reduction of ruby was not based on actual high-pressure experiments with hydrogen, but on a thermodynamic calculation subsequently found to be in error and retracted in a 1993 erratum to the above-mentioned article (Ruoff and Vanderborgh, 1991).

[12]Abrikosov (1954) assumed an ordered hexagonal close packed over the entire range of pressures (see Sec. VI). In recent years, the total energy and electronic structure of hydrogen in this ordered structure has been studied by a large number of groups, as discussed in Secs. VII and XI.

30-GPa range.[13] Most recently, x-ray diffraction measurements have been carried out on hydrogen and deuterium to 42 GPa (Fig. 4) (Mao et al., 1988; Hemley, Mao, Finger, Jephcoat, Hazen, and Zha, 1990; Hu et al., 1994). The two isotopes in Phase I crystallize in the hexagonal-close-packed (hcp) structure. The c/a ratio starts at its ideal value for close-packed spheres (1.633) but decreases continuously with increasing pressure, indicating increasing anisotropy of the crystal (Hu et al., 1994).

The P-V equation of state and the elasticity of the molecular phase provide fundamental data for examining intermolecular interactions, determining potentials, and for testing ab initio theories. Intermolecular potentials developed to model lower pressure properties of hydrogen (<2.5 GPa) are discussed by Silvera (1980). The static high-pressure measurements indicate that all of these potentials fail at high pressures (Hemley, Mao, Finger, Jephcoat, Hazen, and Zha, 1990). Solid hydrogen has been found to be softer (more compressible) than predicted by all previously proposed intermolecular potentials (Fig. 4). On the other hand, one can develop effective two-body potentials $\phi_{eff}(r)$, which are limited to specific properties such as P-V relations.[14] In addition, the data can be fit with phenomenological equations of state. These equation-of-state analyses provide important information on the range of compression of the material to megabar pressures: using the low-temperature zero-pressure density as a convenient reference ($\rho_0 = 0.0435$ mol/cm^3 for H$_2$), for example, 50 GPa corresponds to a compression ρ/ρ_0 of 6; at 150 GPa, $\rho/\rho_0 \approx 9$; and at 250 GPa, $\rho/\rho_0 \approx 11$.[15]

Further information can be obtained by combining synchrotron x-ray diffraction with Brillouin scattering. In the latter technique the diffraction of a laser beam by the grating of a traveling acoustic wave is measured, which yields the compressional- and shear-wave sound velocities. The pressure dependence of the second-order elastic moduli of the crystal can be obtained at each pressure from the Brillouin spectrum with knowledge of the crystallographic orientation determined from x-ray diffraction. Recently, single-crystal elasticity of hydrogen was studied by Brillouin spectroscopy up to 24 GPa at room temperature (Fig. 5; Zha et al., 1993). In addition, fitting both x-ray and Brillouin data has yielded a new effective potential (Duffy et al., 1994), describing the
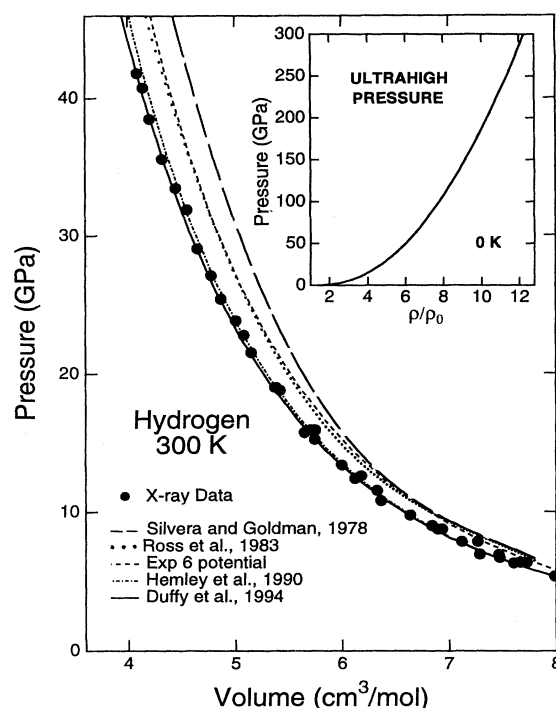

FIG. 4. Pressure-volume relations for solid hydrogen determined from x-ray diffraction at 300 K (Mao et al., 1988; Hemley, Mao, Finger, Jephcoat, Hazen, and Zha, 1990; Hu et al., 1994) compared to equations of state calculated using lattice dynamics from effective pair, or two-body, intermolecular potentials (Silvera and Goldman, 1978; Ross et al., 1983; Hemley, Mao, Finger, Jephcoat, Hazen, and Zha, 1990; Duffy et al., 1994). The potentials and techniques are described in Hemley, Mao, Finger, Jephcoat, Hazen, and Zha (1990) and Duffy et al. (1994). The inset shows the relative density to 300 GPa calculated from a fit to the x-ray data with a three-parameter phenomenological equation of state. The equation of state has the form: $P(X) = 3K_0 X^{-2}[1-X]\exp[\eta(1-X)]$, where $X = (\rho_0/\rho)^{1/3}$ and $\eta = \frac{3}{2}(K'_0 - 1)$; the parameters are $\rho_0 = 0.0435$ mol/cm^3 (the reference molar density), $K_0 = 0.172(4)$ GPa (bulk modulus, K_0), and $K'_0 = dK_0/dP = 7.19(4)$ (pressure derivative of the bulk modulus), all referenced to ambient pressure and to 0 K; only K_0 and K'_0 were adjusted in the fit [see Hemley, Mao, Finger, Jephcoat, Hazen, and Zha (1990)].
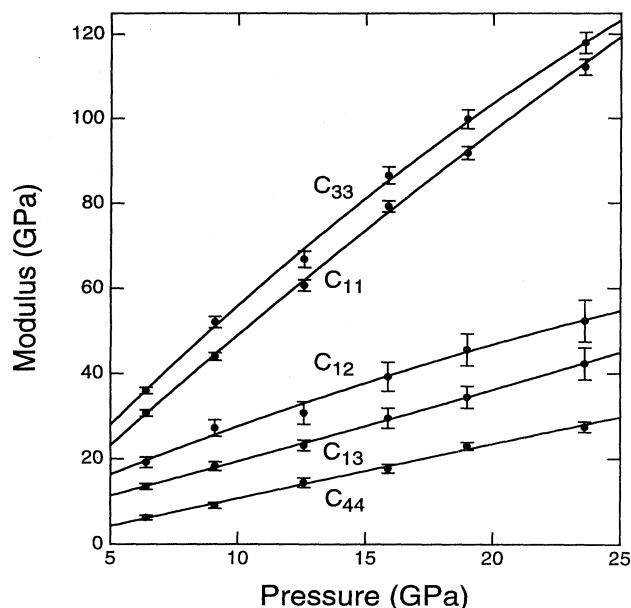
[13]This includes the x-ray diffraction equation of state of H$_2$ and D$_2$ and the neutron study of D$_2$ (Glazkov et al., 1988), the adiabatic decompression study of H$_2$ (Matveev et al., 1984), and the optically determined equation of state of H$_2$ by van Straaten and Silvera (1988a). However, an anomalous isotope effect on molar volume at high pressure (e.g., $\Delta P \approx 8$ GPa at 4 cm^3/mol between H$_2$ and D$_2$) found by van Straaten and Silvera (1988a) is not observed in direct measurements by diffraction (Hemley, Mao, Finger, Jephcoat, Hazen, and Zha, 1990) and arises from inaccuracies in the optical technique.

[14]The effective pair potential designated here is an isotropic representation containing both the orientational effects of the molecules, $\phi_{eff}(r) = \langle \phi(r, \theta, \phi) \rangle$, where the angular brackets denote an orientational average, as well as three-body and higher-order electronic contributions.

[15]The direct measurements to 42 GPa provide an important base for extrapolating the equation of state to multimegabar pressures. Such extrapolations have been useful, for example, for estimating metallization pressures from free-energy calculations, dielectric catastrophes, and dynamic instabilities [see, for example, Mao et al. (1988), Silvera (1989), Ashcroft (1990), and references therein].

FIG. 5. Pressure dependence of the second-order elastic moduli of hydrogen at 295 K determined from Brillouin scattering (Zha et al., 1993). The lines are least-squares fits to the points.

density variation of hydrogen in the megabar region and independently fitting high-P-T shock-wave data well (Nellis et al., 1983). This result has been applied to models of the interior of Jupiter, which contains the bulk of the planetary mass of the solar system (Duffy et al., 1994).

B. Spectroscopic continuity

What is the crystal structure at pressures beyond the range of diffraction techniques, and is there evidence for phase transitions? To address these questions, one can use vibrational spectroscopy, since vibrational excitations can be very sensitive to the crystal structure and degree of orientational order; discontinuous and continuous spectral changes as functions of pressure and temperature are indicative of specific types of transitions in the molecular solid. In the first measurement of the Raman spectrum of solid hydrogen in the diamond cell, Sharma et al. (1980a) found the frequency of the intramolecular stretching mode (vibron) to vary continuously to 60 GPa. Additional constraints were obtained from low-frequency Raman spectra, which have been used extensively at lower pressures to probe the rotational (or librational) excitations as well as lattice modes.

The volume and pressure dependence of the lattice mode (phonon) measured by Raman scattering for H_2 and D_2 is shown in Fig. 6. A remarkably large shift in the phonon frequency is observed, from 36 cm^{-1} at zero pressure $(\rho/\rho_0=1)$ to ~ 1000 cm^{-1} at ~ 150 GPa $(\rho/\rho_0 \approx 9)$. The measurements indicate that the hcp structure, or one based in hcp, is stable over this wide

range, reaching above 100 GPa (Hemley, Mao, and Shu, 1990b; Hemley et al., 1993). Moreover, the phonon frequency is highly sensitive to the form of the intermolecular potential. The dramatic frequency shift of the phonon provides an important test of these potentials, complementary to the equation-of-state measurements. As shown in the insert in Fig. 6, the frequencies calculated by lattice dynamics from the potentials used to describe the equation of state are significantly lower than the measured E_{2g} phonon frequencies for hydrogen.

C. Raman vibron turnover

Sharma et al.'s (1980a) Raman measurements of the vibron revealed something unexpected, however. The vibron frequency initially increased with increasing pressure, normal behavior that results from increasing repulsion between molecules. However, this trend stopped at 30 GPa, above which the frequency decreased with increasing pressure (Fig. 7). This behavior gave rise to considerable excitement in the field, since a decrease in frequency suggests weakening of the intramolecular bond and increased intermolecular interactions, perhaps in anticipation of an eventual transition to a monatomic solid. Subsequently, similar behavior was observed in deuterium, with the vibron turnover occurring at about 50 GPa (Sharma et al., 1980b). Later studies showed the pressure of the vibron turnover in both isotopes to be essentially independent of temperature, although effects of temperature or ortho-para concentration on the frequencies are evident (Wijngaarden et al., 1982; Mao et al., 1985; Hemley, Hanfland, Eggert, and Mao, 1994). Further, measurements to 147 GPa showed that the isotope effect on the vibron shift becomes quite pronounced at ultrahigh pressures (Mao et al., 1985). These observations continued to give rise to conjectures about bond weakening in the solid and its implications for higher-pressure transitions. Ashcroft (1990) showed, for example, that the isotope effect could be rationalized in terms of increasing anharmonicity with pressure, and extrapolating the experimental data predicted dissociation at ~ 300 GPa.[16]

---

[16]In this model the Raman frequencies for the two isotopes were used to determine the parameters of a pressure-dependent intramolecular (Morse) potential (Ashcroft, 1990). The observed isotope effect follows directly from the increasing anharmonicity on the potential, and the instability is reached when the effective dissociation energy vanishes or the phonon frequency reaches the vibron. As is made clear by Ashcroft (1990), the effective potential considered here, being derived from the bottom of the vibron band, contains coupling with the other modes; this is discussed in the following section.

D. Infrared versus Raman vibrons

A deeper and more quantitative understanding of the origin of the vibron turnover was obtained from studying the vibron's dispersion. In general, the internal vibration of a molecule in condensed phase may be coupled with that of other molecules. The vibrational excitation is no longer limited to a single frequency, but dispersed into a range of energy forming a "band." For a given crystal structure there corresponds a well-defined band structure. This is shown in Fig. 8 for the vibron of hydrogen in the hcp structure. Here we use the theory of van Kranendonk (1983), in which the vibron bandwidth is given by $8\varepsilon'$ where ε' is the nearest-neighbor vibrational coupling parameter. The observed Raman vibron ν_R probes the in-phase coupled vibrations of molecules, lying at the bottom of the vibron band, i.e., at $\nu_R = \nu_0 - 6\varepsilon'$, where ν_0 is the frequency of the band origin—the fre-
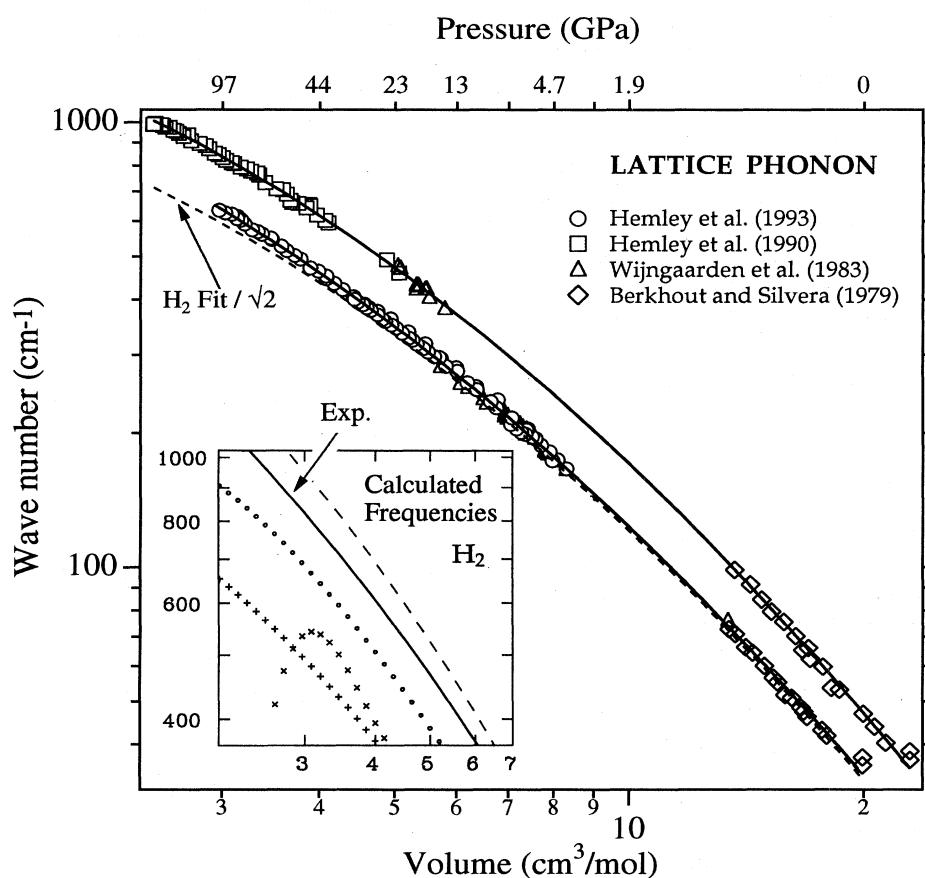

FIG. 6. Volume and pressure dependence of the lattice phonon for H_2 and D_2 probed by Raman scattering: circles, Hemley *et al.* (1993); squares, Hemley, Mao, and Shu (1990); triangles, Wijngaarden *et al.* (1983); diamonds, Berkhout and Silvera (1979). The volume was calculated from the pressure using the x-ray equation of state. The dotted line shows the frequencies expected for D_2 on the basis of the measurements for H_2 in the harmonic approximation. The data of Wijngaarden *et al.* (1983) have been corrected using the x-ray equation of state (Hemley, Mao, Finger, Jephcoat, Hazen, and Zha, 1990). Inset: Comparison of calculated frequency shifts for the E_{2g} mode of hydrogen. The solid line is the experimental curve. The dashed line shows the extrapolation of the earlier fit of Wijngaarden *et al.* (1983). The lower curves show predictions from lattice dynamics calculations using effective potentials (Hemley, Mao, Finger, Jephcoat, Hazen, and Zha, 1990): dotted curve, Silvera-Goldman potential (Silvera and Goldman, 1978); +, modified Silvera-Goldman potential fit to x-ray diffraction data; ×, Exp-6 potential with $\alpha = 11.1$, $\varepsilon = 36.4$ K, $r^* = 3.43$ Å. The result obtained with Exp-6 potential shows the characteristic instability in this function at short range (not evident in the equation-of-state calculation until much higher pressures). At low pressures, the large lattice mode anharmonicity requires the use of the self-consistent phonon-type calculations (Silvera, 1980); however, the lattice mode anharmonicity decreases significantly with pressure so that the quasiharmonic approximation can be used successfully for these properties of the compressed solid.

quency of the uncoupled intramolecular vibration.[17]

At zero pressure, $6\varepsilon'$ is only 3 cm^{-1}, insignificant in comparison to the vibron frequency of 4161 cm^{-1}. This value was thought to remain small at high pressure in the earlier literature; in fact, Wijngaarden et al. (1982) predicted it would vanish under pressure. Hanfland et al. (1992) performed IR measurements on hydrogen to 180 GPa, extending the range of previous work (to 54 GPa) (Mao et al., 1984). These data showed an opposite effect, but one fully consistent with physical intuition: the coupling increases as the molecules are brought closer together. The IR vibron probes the out-of-phase vibration close to ν_0; the difference between IR and Raman vibrons gives a measure of the intermolecular coupling, $6\varepsilon'$ (van Kranendonk, 1983). The IR activity of the vibron in this phase arises from induced interactions. The band origin vibron measured by IR rises continuously without turnover up to 140 GPa (Fig. 7), suggesting that the intramolecular bond is not weakened. Lower pressure IR measurements (Silvera et al., 1992) as well as the Raman studies on isotopic mixtures (Brown and Daniels, 1992; Loubeyre et al., 1992), all below 40 GPa, are consistent with these results. On the other hand, the synchrotron IR measurements demonstrate that above 140 GPa the frequency of the IR band begins to decrease, consistent with the interpretation of bond weakening above this critical pressure. Meanwhile, the intermolecular coupling shows a dramatic increase from 3 cm^{-1} to 500 cm^{-1} in this pressure range, consistent with the Raman vibron turnover (Hanfland et al., 1992).

E. Raman vibron splitting

The increase in intermolecular vibrational coupling has another important consequence, namely, the vibron's assignment at high pressure. At low pressures, a multiplet structure is observed due to splittings arising from molecules in different rotational states. Wijngaarden et al. (1982) assigned the band at high pressure in p-H$_2$ to $Q_1(0)$, claiming together with Silvera et al. (1992) that the splitting between $Q_1(0)$ and $Q_1(1)$ vanished under pressure. Direct measurements indicate instead that the peaks diverge (Fig. 9): the intense vibron that turns over at 30 GPa corresponds to $Q_1(1)$, whereas $Q_1(0)$ tracks the vibron band origin, which increases steeply with pressure (Eggert, Hemley, Mao, and Feldman, 1994). Effects that would show a convergence of peaks, such as rotational averaging (Dion and May, 1973), can be ruled out. Instead, the eigenmodes of a simple model Hamiltonian, calculated by large supercell matrix diagonalizations, lead to predicted Raman line shapes in very good agree-

ment with experimental observations of the Raman active $Q_1(0)$ and $Q_1(1)$ lines up to 10 GPa (Eggert, Hemley, Mao, and Feldman, 1994). Detailed study with these calculations suggests that the major Raman signal corresponds to the Anderson localized states of a binary random alloy in the tight-binding approximation (Feldman et al., 1994).

F. Two-vibron bound-unbound transition

Finally, the large increase in intermolecular coupling has a very interesting and unexpected effect on the vibron overtone region of the spectrum. The overtone region comprises two types of excitations: the first consists of two quanta excited in a single vibron [the overtone $Q_2(J)_{\mathrm{k}}$, $\mathrm{k}=0$]; the second consists of the simultaneous excitation of a single quantum in two separate vibrons with opposite momenta $[Q_1(J)_{\mathrm{k}}+Q_1'(J)_{-\mathrm{k}'}]$, which gives rise
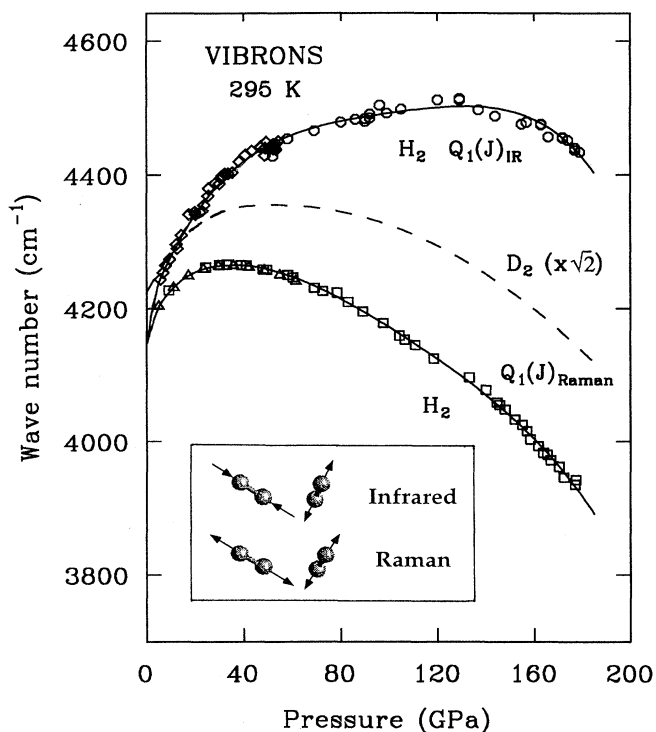

FIG. 7. Pressure dependence of the fundamental transitions of the Raman $[Q_1(J)_{\mathrm{Raman}}]$ and infrared $[Q_1(J)_{\mathrm{IR}}]$ vibrons at 295 K. The Raman and IR vibrons correspond to the in-phase and out-of-phase combination of the two internal stretching modes, respectively, as shown in the inset for an assumed structure (e.g., hcp) with two molecules per unit cell. The Raman data are from Sharma et al. [1980(a)], Hemley and Mao [1990(a)], and Hemley, Hanfland, Eggert, and Mao (1994). The infrared data are from Mao et al. (1984) (low pressure) and Hanfland et al. (1992) (high pressure). The dashed curve summarizes the results for the Raman vibron of deuterium [Sharma et al., 1980(b); Hemley, Hanfland, Eggert, and Mao, 1994], where the frequency has been scaled by $\sqrt{2}$.

---

[17]Alternatively, one can express the coupling in terms of explicit distance-dependent intermolecular potentials, as discussed by Loubeyre et al. (1992).
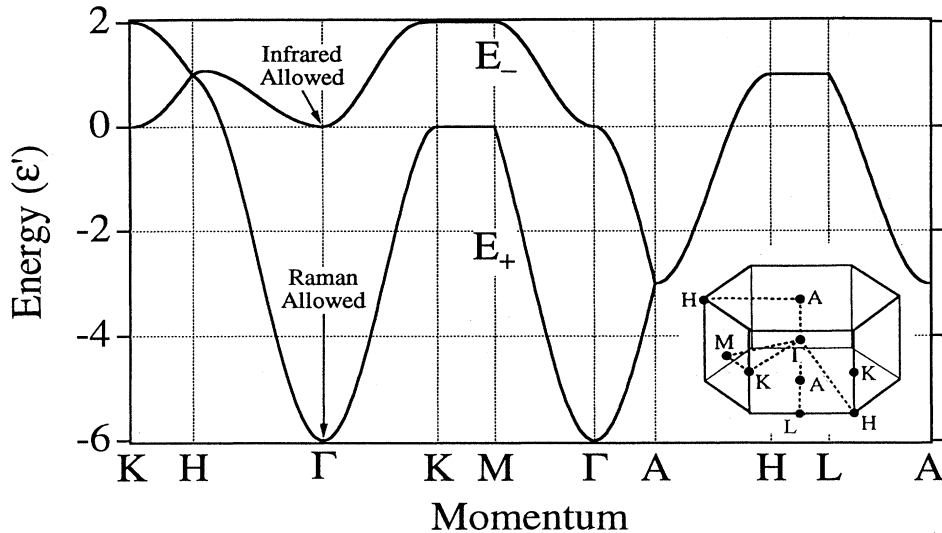
FIG. 8. Vibron band structure for hcp hydrogen calculated assuming only nearest-neighbor interactions. The splitting between the Raman and IR bands equals $6\varepsilon'$ but increases to $7.481\varepsilon'$ if all neighbors are included (Eggert et al., 1993). The inset shows the Brillouin zone for the hcp structure.

to a broad band at higher frequency [Fig. 10(a)].[18] In general, the vibrational dynamics of the overtone have been described successfully by the harmonic approximation for many solids dating back to the early days of solid-state physics. This approximation neglects the anharmonicity of single vibrational excitations, dealing instead with noninteracting phonons in a broad continuum band whose width is a measure of the intermolecular coupling. Anharmonicity prevails, however, in another group of molecular solids that includes hydrogen. Interaction of two phonons leads to the formation of bound quasiparticles separated in energy from the broad continuum. Such a quasiparticle is a biphonon [the bivibron $Q_2(J)_{k=0}$] acting as a molecular oscillator, yielding a sharp peak separated from the origin of the broad two-phonon continuum band by the degree of anharmonicity.

What happens at the transition between the harmonic and anharmonic cases? Kimball et al. (1981) postulated that if the anharmonicity and intermolecular coupling varied so that the anharmonicity became less than the continuum bandwidth, the biphonon would overlap with the band and the bound biphonon would disappear into the unbound continuum band. At the transition the binding interactions of the biphonon would be overcome by intermolecular interactions. Such a transition, however, had never been observed previously by variation of an external parameter (field) in a single system. Pressure provides the ideal means to alter the anharmonicity or the intermolecular coupling and to examine the bound-

unbound transition.

Eggert et al. (1992, 1993; Eggert, Mao, and Hemley, 1994) studied the vibron overtone spectrum of deuterium at high pressures. By the time of these studies experimental sensitivities were greatly improved over those used in 1980 when the fundamental vibron was barely measurable. The new techniques detected the bivibron and the two-vibron continuum with intensities only 10^{-4} and 10^{-5} of the vibron's fundamental, respectively (Eg-
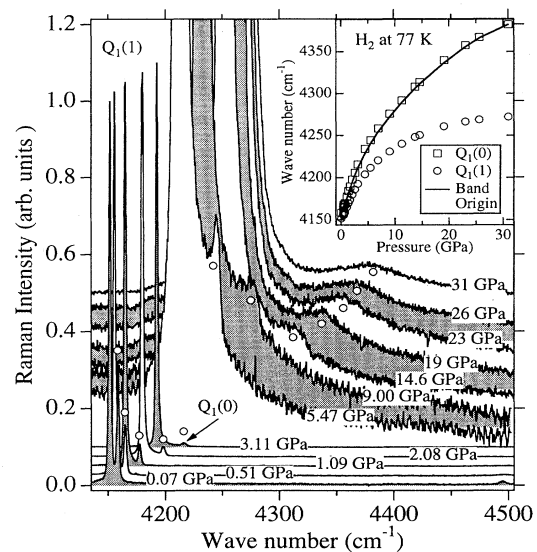

FIG. 9. Raman spectra showing increased splitting of the $Q_1(1)$ and $Q_1(0)$ vibrons with pressure (Eggert, Hemley, Mao, and Feldman, 1994). The inset shows the pressure dependence of the $Q_1(1)$ and $Q_1(0)$ frequencies together with that of the band origin determined from infrared spectra of pure hydrogen (Hanfland et al., 1992; Mao et al., 1984) and Raman spectra of isotopic mixtures (Brown and Daniels, 1992; Loubeyre et al., 1992).

[18]Here we state explicitly the wave vector k of the excitation. The selection rules for Raman scattering require $\sum k = 0$. Thus for the overtone, with a single wave vector, $k = 0$. For excitation on two different molecules, on the other hand, the selection rules require $k = -k'$, which gives rise to a continuous range of excitations.

gert *et al.*, 1992; Eggert, Mao, and Hemley, 1994). As shown in Fig. 10(b), at ambient pressure the anharmonicity amounts to 60 cm^{-1} while the continuum bandwidth is only 2.2 cm^{-1}, whereby the bivibron is well separated from the continuum (Eggert *et al.*, 1993). At high pressures, the anharmonicity remains nearly constant, while the intermolecular coupling increases sharply. The two become equal at 26 GPa, and the bivibron vanishes at 34 GPa above the pressure where the anharmonicity equals the bandwidth due to level repulsion. The results of parameter-free calculations based on a model Hamiltonian agree with the experimentally observed transition (Eggert *et al.*, 1993). It should be pointed out that the bound-unbound transition is not a phase transition but the onset of phonon delocalization. Studying such transitions is an excellent example of the power of pressure control for testing theories of condensed-matter physics.
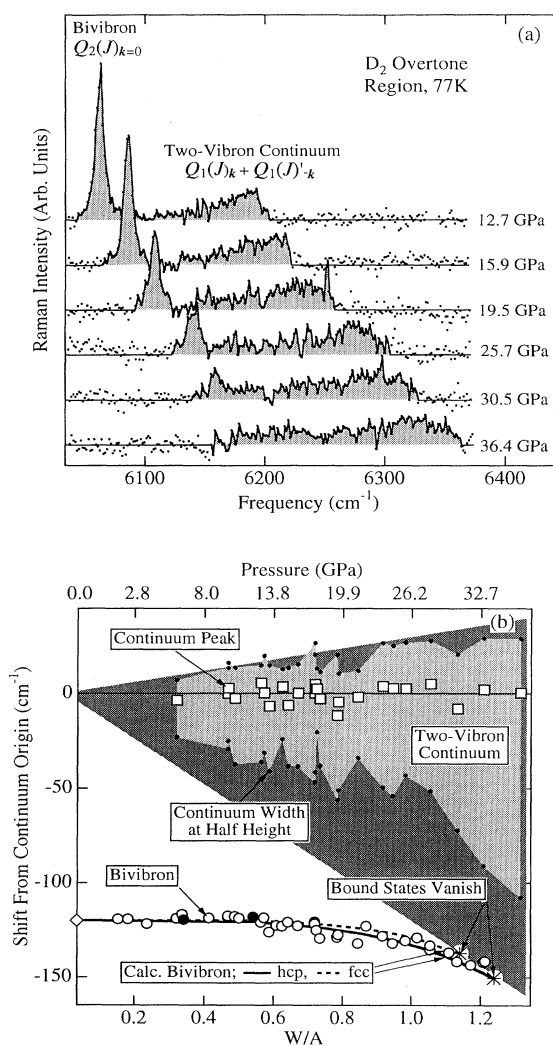

FIG. 11. Predicted oriented crystal structures for hydrogen. (a) cubic *Pa*3 (Silvera, 1989). (b) *c*-axis oriented hcp-type structure (Abrikosov, 1954; Barbee *et al.*, 1989). (c) herringbone structure derived from hcp (Kaxiras *et al.*, 1991). (d) tilted herringbone structure (Ashcroft, 1991a; Kaxiras *et al.*, 1991; Nagara and Nakamura, 1992). Nagara and Nakamura (1992) also considered lower symmetry structures.

VI. PHASE II—LOW-TEMPERATURE SYMMETRY BREAKINGS

A class of molecular phases observed at lower temperatures and high pressures is labelled as Phase II. Transitions from I to II are typically characterized by small discontinuous changes in vibron spectra but larger changes in low-frequency excitations. These transitions arise from lowering of crystallographic symmetry by orientational ordering of the molecules or by structural changes (either reconstructive or displacive). The I-II phase boundaries and the type of ordering depend upon the isotope and ortho-para state. Included in this category are both transitions involving the nominally $J=0$ solids (p-H$_2$ and o-D$_2$) and the ordering transitions (i.e., driven by EQQ) observed at very low pressures (including zero pressure) in ortho-para mixtures. We focus here on the transitions in the higher-pressure range (above 20 GPa).[19]

FIG. 10. Pressure-induced bivibron bound-unbound transition of D$_2$. (a) Raman spectra of D$_2$ in the overtone region as a function of pressure. (b) Comparison between experimental results and model Hamiltonian calculations for the transition (Eggert *et al.*, 1993).
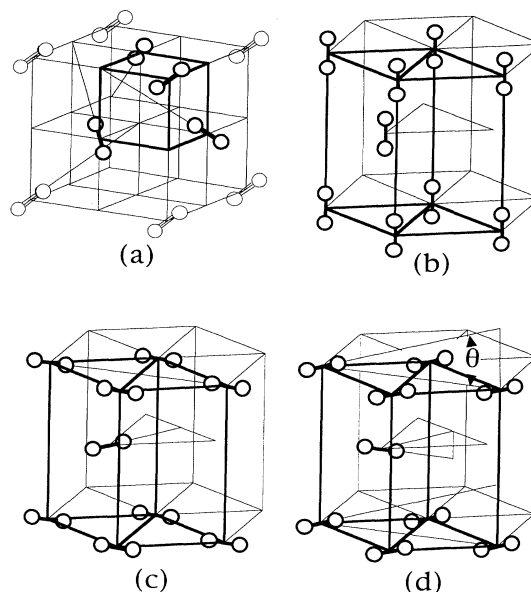
---

[19]The I-II transitions at high pressures are reported on the basis of observations of new peaks or changes in frequencies or intensities of Raman or IR spectra. However, the signatures for the transitions in o, p, and n hydrogen and deuterium vary considerably. Because their crystal structures in the Phase-II region have not been directly determined at high pressures, it is still uncertain whether they all have the same structure or structures.

High pressure breaks the rotational symmetry of the $J = 0$ solids by mixing higher rotational levels into the ground state, thereby leading to the electric quadrupole-quadrupole transition. At low temperatures (below 10 K), the molecular ordering transition was reported in o-D_2 at 28 GPa (Silvera and Wijngaarden, 1981) and in p-H_2 at 110 GPa (Lorenzana et al., 1990). Recent Raman and infrared measurements provide evidence for a new transition (or several transitions) beginning at 65 GPa at 77 K (Hemley et al., 1993). Spectroscopic measurements provide constraints on possible structures when low-frequency vibrational spectra can be measured (Hemley, Mao, and Shu, 1990; Hemley et al., 1993). A variety of ordered phases have been proposed, all of them derived from either hexagonal- or cubic-close packing (Fig. 11).[20]

Infrared absorption spectroscopy has revealed a transition in n-H_2 at 110 GPa and 85 K (Figs. 12 and 13). At higher pressure or lower temperature, a new, sharp vibron appears 45 cm^{-1} below the old vibron. The additional vibron indicates that the ordered Phase II has lower symmetry than hcp, which can have only one (induced) IR vibron. Recent work indicates that the boundary between I and II for both n-H_2 and n-D_2 has a small positive dT/dP slope (Li et al., 1994; Hemley, Goncharov, Eggert, Hanfland, and Mao, 1994) and a triple point (see below). Among the proposed ordered structure (Fig. 11), the structure with molecules aligned along the c axis of the hcp structure (Abrikosov, 1954) can therefore be rejected. The $Pa3$ structure seems unlikely on the basis of the evidence for continuity of the E_{2g} phonon in the Raman spectrum (Hemley, Mao, and Shu, 1990). Certain flat or tilted herringbone structures, lowering the hcp symmetry (Kaxiras et al., 1991; Nagara and Nakamura, 1992), are acceptable.[21]

VII. PHASE III—THE 150-GPa TRANSITION

Measurements at still higher pressures reveal another high-pressure phase—Phase III. The transition is characterized by marked changes in Raman and IR spectra of hydrogen at 150 GPa and low temperature (< 140 GPa). The transition is especially intriguing because a variety of theoretical calculations predict valence-

---

[20]The transitions may be sluggish and spread out over a wide pressure interval. It has been suggested that the transitions could be martensitic, involving mixed stacking of close-packed layers in a mixed-phase region (Hemley et al., 1993). This then would be analogous to the metastable coexistence of fcc-hcp phases observed at low pressures (Schuch et al., 1967).

[21]It is also possible that rotational disorder may be frozen in at these pressures; that is, producing static orientational disorder akin to a spin glass. Indeed, this could be similar to the quadrupolar glass documented for hydrogen at low temperatures and ambient pressure where the EQQ interactions dominate (Sullivan et al., 1978).
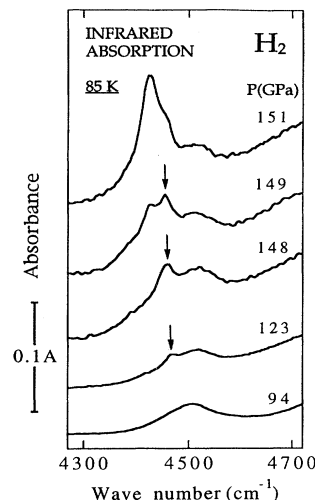

FIG. 12. Infrared absorption spectra as a function of pressure at 85 K showing evidence for the low-temperature transition at 110 GPa (Hanfland et al., 1993). The arrow identifies the sharp vibron peak near 4465 cm^{-1} diagnostic of Phase II. The stronger band at 4425 cm^{-1} appearing at higher pressures arises from the partial transformation to Phase III beginning at ~150 GPa. The absorbance (optical density) is given by the vertical scale bar.
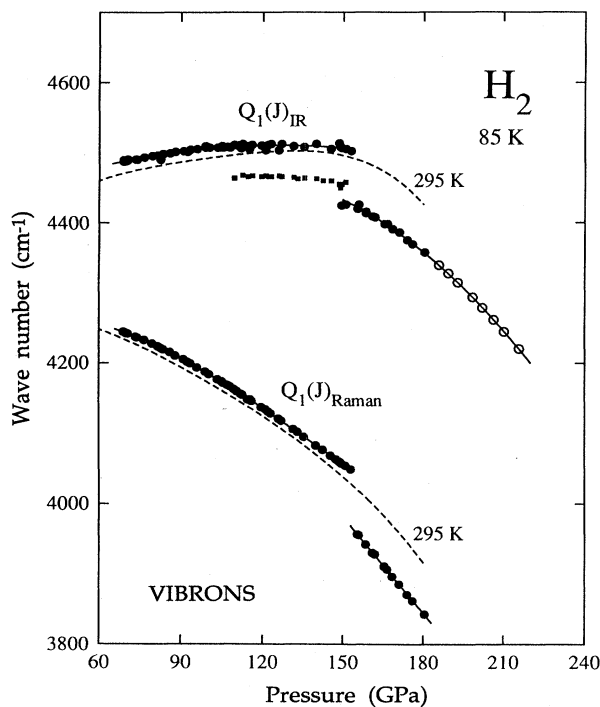

FIG. 13. Pressure dependences of the Raman and infrared vibron frequencies $[Q_1(J)_{Raman}]$ and $[Q_1(J)_{IR}]$ showing the I-II and II-III phase transitions. The 295-K data (Phase I) are given by the dashed curves (Hanfland et al., 1993).

conduction band-gap closure in the molecular solid in this pressure range. A large number of experiments have now been performed in an attempt to understand the new phase.

A. Raman vibron discontinuity

Phase III was discovered by the observation of an unprecedented discontinuity of the Raman vibron of n-H_2 (Hemley and Mao, 1988). When pressure was raised above ~ 150 GPa at 77 K the original vibron disappears, being replaced by a new vibron 100 cm^{-1} below the old one (Fig. 14). Previous phase diagrams for p-H_2 and o-D_2 (Silvera, 1989) suggested that the transition could be an extension of the low-pressure EQQ molecular ordering transition. Alternatively, it could be a totally new orientational transition. Hemley and Mao (1988) pointed out that the transition P-T point (77 K and 150 GPa) did not exactly fit the expectation for pure EQQ interactions, raising a need for a more complete model. To test this, we examined n-D_2. Since the rotational constant in D_2 is half that of H_2, molecular ordering transitions should occur more easily in D_2; that is, at a lower pressure. We monitored the intramolecular vibron as a function of pressure at 77 K, observing that the D_2 went through the same vibron discontinuity transition at comparable pressures. We concluded that the transition is not a simple EQQ ordering transformation, but is consistent with a new type of transition. This conclusion was also reached by Lorenzana et al. (1989) on the basis of measurements of the temperature dependence of the transition.

The vibron discontinuity decreases with increasing temperature as shown for H_2 in Fig. 14. This observation
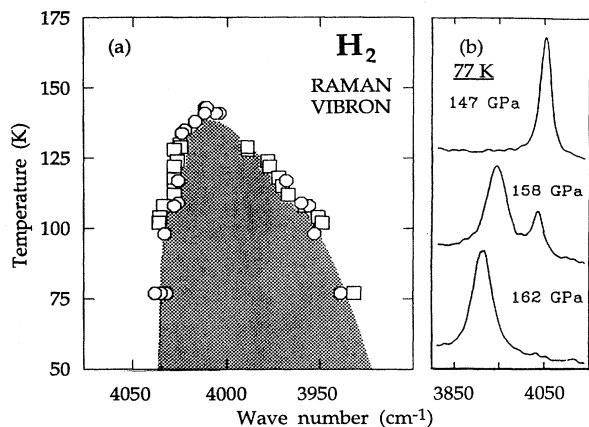

FIG. 14. Raman vibron at the 150-GPa transition (Hemley and Mao, 1990). (a) Temperature dependence of the two vibron frequencies during coexistence of the two phases in the sample (Phase II-III or I-III). The squares are results reported by Lorenzana et al. (1989). The pressure varies from 150 to ~ 167 GPa from low to high temperature in the figure. (b) Representative Raman spectra as a function of pressure ($T = 77$ K) showing phase coexistence at 158 GPa.

suggests the presence of a critical or tricritical point (Landau, 1935), above which temperature the discontinuous phase transition becomes continuous. The existence of a critical point would place a strong constraint on possible types of phase transitions. The transition would have to be one in which Phase III can be derived from Phase I through both continuous and discontinuous routes. For instance, this would rule out transitions involving reconstruction of the crystal structure. Either molecular orientational transitions or electronic transitions (or both) satisfy the available experimental constraints; both have been predicted by independent theoretical studies (Barbee et al., 1989; Garcia et al., 1990; Chacham and Louie, 1991; Kaxiras et al., 1991; Surh et al., 1993). The vibron discontinuity in D_2 has been studied with high resolution and accurate temperature control (Hemley, Goncharov, Eggert, Hanfland, and Mao, 1994). Although it also decreases with increasing temperature, a phase boundary has been detected to at least 270 K. Direct tests are in progress for distinguishing among alternative hypotheses of a critical point, tricritical point, or first-order transition with a small vibron discontinuity.

B. Optical measurements

In the conventional one-electron approximation, band-overlap metallization occurs when the top of the valence band crosses the bottom of the conduction band. If this overlap occurs at a different point of the Brillouin zone (indirect band gap), one initially has a semimetal, i.e., a metal with low electron carrier density. The dielectric properties of hydrogen are controlled in part by excitations at and above the direct band gap, and can be monitored from measurements of its refractive index as a function of frequency in the diamond cell (van Straaten and Silvera, 1988b; Eggert et al., 1990; Eggert, 1991; Hemley et al., 1991; Garcia et al., 1992). The hydrogen sample confined by two parallel diamond surfaces forms a Fabry-Perot interferometer. Visible and infrared radiation that is passed through the sample and multiply reflected by the two hydrogen-diamond interfaces produces an interference pattern according to the Airy equation, which yields the refractive index as a function of frequency for hydrogen, $n_H(\omega)$ [Fig. 15(a)].

Such index-of-refraction measurements have been particularly useful for constraining the pressure dependence of the dielectric function of hydrogen with simple single-oscillator models for the high-energy electronic excitations (i.e., above the band gap). The measurements can be used to study the ultraviolet spectrum, which is inaccessible because of stress-induced absorption by the diamond anvils. A linear decrease in the frequency ω_1 of the oscillator with increasing density was found, in agreement with electronic structure calculations [Fig. 15(b)]. Recent determinations of the band gap from electrical conductivity measurements of shocked fluid hydrogen

(Nellis *et al.*, 1992) are also very close to both the theoretical and static compression curves for the solid. The refractive index measurements indicated that direct gap closure requires pressures above 300 GPa (Hemley *et al.*, 1991). Although the direct gap is reduced substantially with increasing pressure, it remains above ~ 3 eV at the I-III boundary. If the transition corresponds to band-gap closure, the gap must be indirect, giving rise to a system with a low carrier density ($\omega_p < 0.5$ eV; Hanfland *et al.*, 1991).

The visual transparency of hydrogen III does not necessarily preclude metallization, since hydrogen could be an unusual metal with a Drude edge in the IR range. In the free-electron Drude model, a metal is defined by the existence of a plasma frequency edge separating the low-frequency opaque and reflective region and the high-frequency transparent and nonreflecting region. Reflectivity and opacity change sharply at the edge. Using a conventional IR spectrometer, Mao *et al.* (1990) first measured reflectance of high-pressure hydrogen to 177 GPa at 295 K in the frequency range from 24 000 to 4000 cm^{-1} (3 to 0.5 eV), observing a 4% rise of reflectance at the IR limit (4000 cm^{-1}). The rise could be modeled as part of a Drude excitation (in a simple one-band model) with the highly reflective portion hidden in the lower-frequency region, which was inaccessible with available measurement techniques. Subsequent transmission studies, however, showed a significantly weaker absorbance of the sample than predicted by a Kramers-Kronig transform of the reflectance data (Hanfland *et al.*, 1991; Eggert *et al.*, 1991). Although this could indicate a failure of the Drude model, this finding motivat-
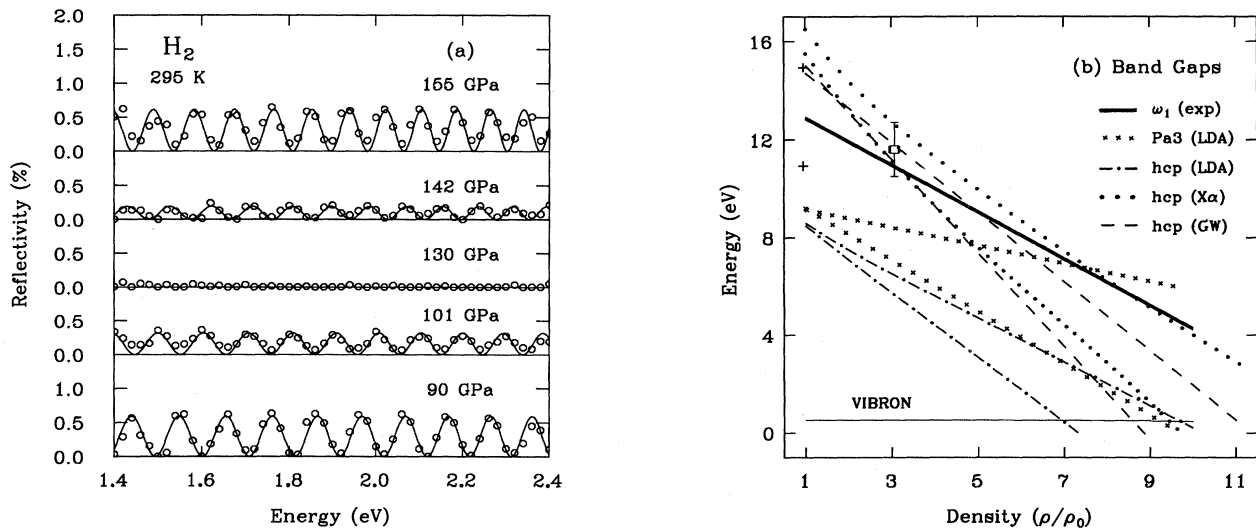

FIG. 15. Results of high-pressure dielectric measurements for hydrogen. (a) Visible light interference patterns at 295 K (Hemley *et al.*, 1991). The solid lines correspond to simultaneous fits of the Airy equation for a Fabry-Perot interferometer and a single-oscillator model for the dielectric properties (e.g., index of refraction). The Airy equation is given by $I_R(\omega)/I_0(\omega)=1-1/[1+F\sin^2(\omega\delta/c)]$, where $F=4R/(1-R)^2$ and is a measure of the amplitude of the fringes, and R is the reflectivity given by the Fresnel equation, $R=(n_d-n_H)^2/(n_d+n_H)^2$, c is the speed of light, and $\delta=2n_H d\cos\theta$, where d and θ are the samples of thickness and angle of the incident light, respectively. The single-oscillator model for the refractive index is expressed as $n_H(\omega)-1=F_1/(\omega_1-\omega)^2$, where F_1 is the oscillator strength and ω_1 is an effective oscillator correlating closely with valence-conduction band electronic transitions (Eggert *et al.*, 1990, Hemley *et al.*, 1991). The decreased amplitude of the fringes at 130 GPa indicates that $n_d\approx n_H$ at this pressure. (b) Comparison between experiment and theory for the density dependence of effective band gaps. Both the experimentally determined ω_1, shown by the thick line, and the theoretical curves are linear functions of density (Hemley *et al.*, 1991). The crosses correspond to the lowest-energy exciton and the estimated band gap at ambient pressure ($\rho/\rho_0=1$). The square shows the shock-wave determination of the band gap for fluid deuterium (Nellis *et al.*, 1992). The lower and upper curves for the hcp calculations correspond to ordered and disordered structures calculated using the LDA and X_α methods (Garcia *et al.*, 1990) and the GW technique (Chacham and Louie, 1991). The upper (lower) curve for $Pa3$ is the direct (indirect) gap calculated by Friedli and Ashcroft (1977). The behavior of ω_1 at the highest pressures is consistent with both the appearance of visible absorption above 250 GPa and the observations of resonance enhancement of the Raman vibron (Mao and Hemley, 1989). The single oscillator model begins to break down, however, when ω_1 approaches the probe energy. The density dependence of the vibron frequency is indicated by the thin line.

ed the development of new techniques to test alternative hypotheses,[22] including the contributions of vibrational excitations to the optical spectra.

C. Synchrotron IR studies

With the development of Fourier transform infrared (FTIR) spectroscopy employing synchrotron radiation, major advances have been made in resolution, sensitivity, and frequency range of IR absorbance measurements. We now have a much better understanding of hydrogen IR vibrational peaks in Phase III. The corresponding reflectance measurement technique for testing the above hypotheses is under development. As in the Raman measurements, the IR vibron shows a low-temperature discontinuity (Fig. 13; Hanfland et al., 1993). The frequency discontinuity in the IR coincides with that in the Raman spectrum. In Phase III, the IR vibron frequency decreases with increasing pressure, indicating that the discontinuous frequency drop in the II-III transition reflects softening of the intramolecular vibration, rather than a strengthening of intermolecular coupling; the softening continues in Phase III.

The IR bands arising from rotation excitations (vibron plus roton combination bands) change abruptly above the II-III transition (Fig. 16), an observation consistent with a change of molecular orientation involving an appreciable symmetry breaking. These changes are significantly larger than those observed at the I-II transition at 110 GPa (85 K). As in the Raman measurements (Hemley, Mao, and Shu, 1990), the IR lattice phonon frequency seems to shift continuously from Phase II to III, suggesting similar lattice structures in both phases. The vibron-phonon combination band $[Q_R(J)]$ is measured in the infrared absorption spectrum, $Q_R(J)-Q_1(J)$ appearing close to the B_{2g} (LO) lattice mode (Fig. 3). In contrast, the doubly degenerate E_{2g} (TO) mode is active in the Raman spectrum (assuming a structure close to hcp). The large difference between the IR and Raman phonons of

---

[22]The following hypotheses were proposed by Hanfland et al. (1991): (1) The sample was optically and electronically anisotropic. A higher reflective thin film of hydrogen grown epitaxially on the diamond surface had different crystallographic orientation and optical properties from the bulk hydrogen sample. The reflectance, which is controlled by the hydrogen/diamond (H/d) interface, would not correlate with bulk sample absorbance. (2) The refractive index of diamond at the anvil tip increased sharply at 150 GPa, thus affecting the H/d interfacial properties. Such changes could arise from penetration of hydrogen into the tip of the anvil. (3) The rise of reflectance in the IR was not due to a Drude edge, but to a sudden intensification of vibrational peaks, which appeared as an edge within the limited spectral range and resolution of the measurements.
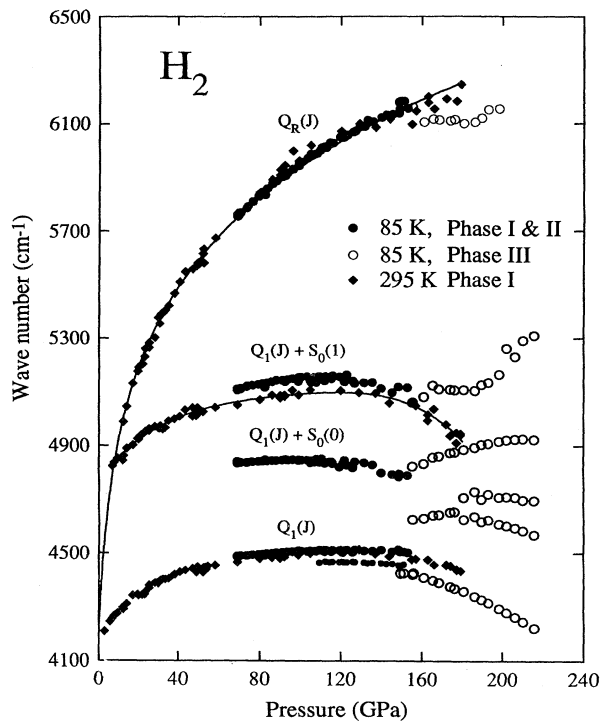
FIG. 16. Pressure dependence of the IR bands measured at 85 K. The $Q_1(J)$ vibron band is indicated. The higher-frequency bands arise from excitations of one quantum in the vibron and one in either a rotational or a lattice phonon. The $Q_R(J)$ band designates excitation of the vibron in combination with a lattice phonon (Hanfland et al., 1994). Above 150–160 GPa, the pressure shifts of the vibron-rotational combination bands change distinctly, indicative of a major symmetry breaking.

Phase III (LO-TO splitting $= 700$ cm^{-1} at 160 GPa) suggests a possibly large elastic anisotropy as well.

D. IR vibron absorption

The most striking feature observed in high-pressure hydrogen is the enhancement of IR vibron absorption in Phase III. This result is of particular interest in view of the fact that absorption corresponding to the intramolecular stretching mode vanishes in the free molecule! The absorbance maximum of a 3-μm thick hydrogen sample increases from 0.02 in Phase II at 150 GPa to 3.0 in Phase III at 175 GPa (Hanfland et al., 1993). The absorbance of 3.0 implies a transmission signal of 10^{-3} of the incident beam, which reaches the saturation limit of the instrument. Calculations of the oscillator strength (Hemley, Soos, Hanfland, and Mao, 1994), which measures the integrated intensity of the band, showed that the absorption continues to increase in the high-pressure phase (Fig. 17).

The intensity of IR absorption A is a measure of the electric dipole moment μ generated in a transition be-
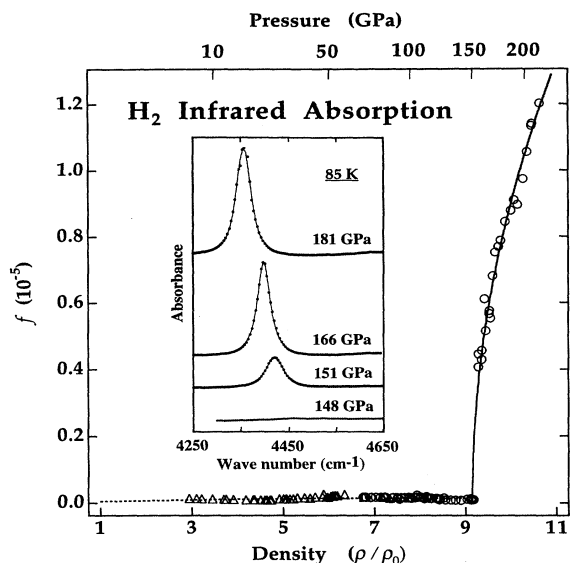
FIG. 17. The increase in IR vibron absorption at the 150-GPa transition given as the oscillator strength as a function of density and pressure (85 K). The oscillator strength is defined as $f = 4.315 \times 10^{-9} \int \varepsilon(v) dv$, where $\varepsilon(v)$ is the molar extinction coefficient (in $\mathrm{cm}^{-1} \mathrm{mol}^{-1}$ liter) given by $\varepsilon(v) = \log(I_0/I)/(cl)$, c is the concentration in mol liters^{-1}, l is sample thickness, and I and I_0 are the intensities of the transmitted and incident light, respectively, on the sample. The inset shows the measured spectra of the vibron at the transition.

tween the two states i and j, $A \propto |\langle i|\mu|j\rangle|^2$. In the ground electronic states, isolated homonuclear diatomic molecules such as H_2 possess no permanent electric dipole moment because they have a center of symmetry; excitation of the intramolecular stretching mode in the isolated molecule is thus IR forbidden. In the solid phase, weak electric dipole moments are induced by intermolecular interaction (van Kranendonk, 1983). The absorbance of the hydrogen IR vibron increases with the square of density, but its maximum is still less than 0.02 at 150 GPa (Hanfland et al., 1992) (relative density $\rho/\rho_0 = 9$), indicating that despite the monotonic increase in intermolecular vibrational coupling (Hanfland et al., 1992), the basic electronic properties change only moderately with pressure in Phases I and II. However, a large increase in the transition moment of the IR vibron occurs in Phase III. The transition dipole approaches that of an OH stretching vibration in an isolated water molecule.

VIII. PHASE IV?—BEYOND 250 GPa

Mao and Hemley (1989) reported optical studies of hydrogen samples smaller than 3–5 μm to pressures above 200 GPa, the region where direct band-gap closure and molecular dissociation were predicted. The experiments indicated that hydrogen begins to absorb visible light with increasing pressures above 250 GPa. Because of the

small sample size and the sharp increase of diamond fluorescence at ultrahigh pressures, the ruby R_1 peak used for pressure calibration was very weak and difficult to measure above 230 GPa. The pressures reported above 250 GPa were the minimum values estimated from the force applied to the diamond anvils.

Visible spectra showed increasing absorption above 250 GPa (Mao and Hemley, 1989), consistent with band-gap dielectric model fits to the index-of-refraction measurements shown in Fig. 15 (Hemley et al., 1991). Observation of the molecular Raman vibron in Phase III above 200 GPa indicated that molecular bonds are stable to at least $\sim$230 GPa above which the Raman vibron could not be detected. Disappearance of the Raman vibron is consistent with molecular dissociation; this is, however, a necessary but not sufficient condition for dissociation. The disappearance could also have been caused by the pressure-induced absorption of the exciting laser, by the fluorescence of the diamond and the sample, or by loss of hydrogen to the anvil. A new low-frequency Raman peak was observed in later studies of both isotopes at pressures of 150–200 GPa (Hemley and Mao, 1992; Hemley et al., 1993). The new peak may be associated with hydrogen penetration into the tip of the diamond anvil (chemical effect), various properties of the hydrogen-diamond interface, or a nonvibrational excitation in bulk hydrogen.

The transition pressure to the theoretically predicted high-density plasma state, the nonmolecular quantum metal, is not known and thus its properties have yet to be established experimentally. However, the static pressure experiments provide a lower bound for the transition of $\sim$250 GPa. Theoretical calculations continue to predict unique properties of this phase or phases (Barbee et al., 1989; Natoli et al., 1993). Theoretical studies differ widely in their prediction of the range of stability of the molecular phase (Barbee et al., 1989; Ashcroft, 1990; Nagara and Nakamura, 1992). In the search for this transition, it is encouraging that as early as 1989 the ultrahigh-pressure study of hydrogen was limited by measurement sensitivity rather than by the maximum attainable pressure.

IX. AN EMERGING PARADIGM

A. Intermolecular vibrational coupling

The growing body of data for hydrogen as a function of pressure shows it to be an intriguing system characterized by competition between orientational ordering, closing of the band gap, and destabilization of the paired state. The strong intermolecular coupling provides a consistent explanation of the observed changes in spectroscopic properties, including such phenomena as the bound-unbound bivibron transition and the vibron turnover. But identification of the coupling begs the question of the interaction's origin: are they principally EQQ, van

der Waals, or exchange-type? To what extent can they be ascribed to charge transfer? Further, the relative contributions of two-body intermolecular and many-body (two-body atom-atom and higher-order) interactions need to be addressed. Hanfland *et al.* (1992) showed that the difference between the IR and Raman frequencies for the vibron $[Q_1(J)_{IR} - Q_1(J)_{Raman}, 6\varepsilon'$ in van Kranendonk's model] increases as R^n with $n = 6.89$ (± 0.05), where R is the intermolecular distance calculated from the x-ray equation of state. Effects arising from a dipole-induced dipole (leading-order van der Waals) interaction would increase as R^6. This similarity suggests that van der Waals interactions continue to make the major contribution; however, the determination of $n > 6$ may be significant, and other interactions are likely to be dominant at the highest pressures.

The inadequacy of pair-potential models for the equation of state and the lattice phonon is a related problem (Hemley, Mao, Finger, Jephcoat, Hazen, and Zha, 1990). For example, the poor agreement between the measured lattice mode frequencies and those calculated from these same potentials (Fig. 6) indicates the need for a more elaborate treatment of the intermolecular interactions. Detailed treatments of polarizability expansions indicate both the higher-order terms *and* many-body contributions are important in condensed phases (Doran and Zucker, 1971); in general, the two-body description represents an effective interaction (and in part could obscure the underlying physics of the problem). A similar point has been echoed by Maggs and Ashcroft (1987), who have emphasized the inadequacy of two-body polarizability models for describing the interactions in dense polarizable systems.

B. I-II-III triple point

The relationship between the I-II and II-III boundaries has recently been examined in higher resolution Raman and IR experiments with accurate temperature and pressure control. The I-II transition is characterized by the presence of multiple IR vibrons and a small but detectable discontinuity in the Raman vibron. The II-III and I-III transitions are characterized by discontinuities in Raman and IR vibron frequencies, the IR vibron intensity change, and IR roton-viron combination spectra. For both H_2 and D_2, the three phases and transition boundaries intersect at an invariant triple point. The phase diagram for D_2 is shown in Fig. 18. It is interesting to note that the topology is similar to that associated with a Mott transition (Mott, 1990), in which there is an electron spin-ordered antiferromagnetic phase (for hydrogen, Phase II) at low temperatures, a disordered phase at high temperatures, an electron delocalized phase at high pressure, and a triple point.

C. The nature of Phase III

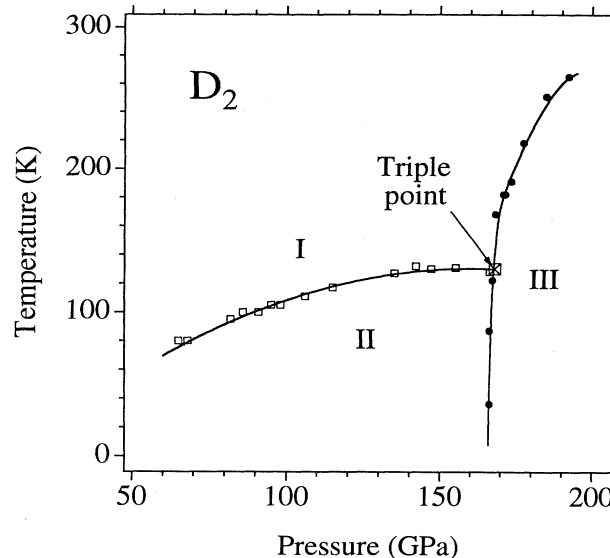In 1989, Hemley and Mao pointed out the consistency of the transition to Phase III involving structural as well

FIG. 18. Phase diagram for n-D_2 at megabar pressures. Phases I, II, and III meet at an invariant triple point, at 167(± 8) GPa and 129(± 3) K, based on recent preliminary measurements. The data points correspond to Raman and infrared measurements of the phase lines, including those reported by Hemley *et al.* (1993). Further details are given by Hemley, Goncharov, Eggert, Hanfland, and Mao (1994). Similar results have been obtained for H_2 (Li *et al.*, 1993).

as possibly electronic changes—still a broad hypothesis requiring further constraints. The study of lattice phonon spectra confirmed that the crystal structure with respect to molecular centers is related to hcp (Hemley, Mao, and Shu, 1990). The observation of a rise in reflectivity in the 4000–5000 cm^{-1} range at 177 GPa was at first modeled as a simple Drude feature. However, the absence of absorption in the same frequency and pressure range (Hanfland *et al.*, 1991), and in a different experiment (Eggert *et al.*, 1991) in the 5000–10000 cm^{-1} range and to 230 GPa, modified the simple Drude hypothesis to include the three hypotheses listed above. The study of dielectric properties ruled out direct bandgap closure. Most recently, the observation of a sharp increase in transition moment for the vibron, together with a discontinuity in the vibron frequency, shows there is indeed another, and much more dramatic, symmetry breaking upon passage into Phase III.

The IR and Raman roton spectra suggest that molecular orientational ordering in Phase III changes abruptly from that of Phase II, evidence for further symmetry breaking. At this point, one expects the low-pressure single-molecule ortho-para distinction to be lost. However, a major question remains concerning the extent to which this approximation breaks down below 150 GPa as rotational motion is hindered and intermolecular interactions increase. Phase I is likely to order gradually and to

be partially ordered prior to the 150-GPa transition (Hemley, Mao, and Shu, 1990), transforming continuously to Phase III (i.e., above a critical temperature). The ordered structures and the ordering mechanisms could be different in all three phases. Moreover, the IR data shown above (Fig. 16) show evidence for additional transitions, as do the earlier Raman measurements (Lorenzana et al., 1990; Hemley and Mao, 1992).

D. Role of charge transfer

Increasing density may enhance the charge transfer between molecules, whose effect on various properties of hydrogen has been mentioned in a variety of contexts but until recently never examined in detail. Interestingly, the onset of intense IR vibron absorption at 150 GPa seems to parallel the spectral properties of organic charge-transfer (CT) salts, including pressure-induced neutral-to-ionic transitions (Hanfland et al., 1988; Bozio and Pecile, 1991). The dramatic rise in absorption reflects the increase of vibronic (electron-vibron) coupling between a charge-transfer electronic transition and the vibron. The salient features of the mechanism can be adduced from a dimer model (e.g., isolated H_2H_2). With increasing electron overlap of the molecular wave functions, charge-transfer states can mix with the ground state. Such mixing is, however, strongly dependent on the relative orientation of the molecules (Hemley, Soos, Hanfland, and Mao, 1994). The admixture allows IR vibron intensity to be "borrowed" from the charge-transfer band. Quantitative calculations can rationalize not only the magnitude and equality of the IR and Raman vibron discontinuities but also the extraordinary IR absorption as a function of the density of Phase III. Moreover, the charge-transfer excitation is predicted to track closely the effective oscillator frequency of hydrogen derived from measurements of the refractive index (Hemley et al., 1991; Eggert, 1991). In this regard, it may be useful to consider the consequence of the energy of the indirect band gap reaching the frequency of the vibron under pressure (i.e., ~0.5 eV; Fig. 17). Under such conditions, one may expect to find large enhancements of electron-phonon (electron-vibron) coupling.

E. Band-gap closure and proton dynamics

But does the band gap close under pressure? Theoretical calculations show the pressure of electronic band-gap closure to depend strongly on crystal structure, the assumed molecular orientation, and the level theory that is used [Fig. 15(b)]. Local-density-approximation (LDA) calculations of c-axis ordered phases predict band-gap closure as low as 40 GPa (Barbee et al., 1989), in part as a result of the underestimate of the gap at this level of approximation. Chacham and Louie's (1991) quasiparticle calculations, which go beyond the LDA, appear to provide much better estimates of the band gap for a given

structure. Considerable theoretical effort has been made to determine the lowest-energy ordered structure under pressure (neglecting dynamical, including quantum, effects). An important conclusion is that lower-energy ordered structures preserve the valence-conduction band gap to higher pressures (even beyond 150 GPa) and that the gap is not necessarily reduced by orientational order (Kaxiras et al., 1991). Nagara and Nakamura (1992) calculate that the molecule's potential at high pressure parallels that of an electric quadrupole, predicting that the ordering transitions should therefore be similar at high and low pressures. Kaxiras et al. (1991) proposed a new class of ordered, tilted-herringbone structure, agreeing with available structural and electronic constraints. A significant effect of zero-point motions on the metallization pressure has been predicted recently (Surh et al., 1993), and quantum effects on the structure have been examined in large-scale molecular dynamics simulations (Hohl et al., 1993).

Other calculations that go beyond the standard assumptions of a perfect crystal and a one-electron approximation for the band structure suggest further possibilities. Ordinarily band-gap closure implies metallization, and thereby an opaque and reflective sample. Since Phase III is colorless and transparent in the visible (<250 GPa), several mechanisms have been proposed to avoid metallization, or to delay it to higher pressures. One hypothesis calls for quantum motions of the nuclei decreasing the mean free path of electrons, perhaps forming an insulator as a result of Anderson-type localization arising from dynamic (Ashcroft, 1991b) rather than static disorder (Anderson, 1958). Apparently such localization has not been observed previously in a crystalline material. The presence of static orientational disorder (orientational glass) in hydrogen could also give rise to localization. Another hypothesis calls for conduction electrons bound to holes forming an excitonic insulator below a critical temperature (Hemley and Mao, 1990). If the electrons remain localized, then the insulating molecular phase may transform directly to a nonmolecular metallic phase. We emphasize that these hypotheses remain to be tested by further high-pressure experimentation. Mott (1990) has pointed out that unusual electronic effects are often found near points of band overlap.[23] It is intriguing to speculate that some of the anomalous Raman scattering observed above 150 GPa, including both sharp low-frequency bands (Hemley and Mao, 1992) and the diffuse

---

[23]The situation appears to be even more interesting in the case of hydrogen. Moulopoulos and Ashcroft (1991) raise the possibility that in the band-overlap molecular metal there may emerge new ordering schemes involving pairing of protons (covalent bonding), electrons and protons (the excitonic states), and electrons themselves (Cooper pairs). Owing to the highly dynamic character of the system, the breakdown of the Born-Oppenheimer approximation may introduce additional new physics.

signal (Hemley, Mao, and Shu, 1990; Hemley *et al.*, 1993), may be electronic in origin, but this requires further study.

X. FUTURE PROSPECTS

Major progress has been made in the past five years in understanding the unique properties of hydrogen at very high densities, owing to the significant progress in experimental ultrahigh pressure techniques based on the diamond-anvil cell. Work on hydrogen in particular and the development of general high-pressure techniques motivate and enhance each other, helping to provide continuous developments in both. New discoveries present new questions requiring new tests, including further structural and optical measurements and perhaps direct measurements of electric conductivity or magnetic susceptibility of hydrogen at ultrahigh pressures. This includes studies of the system at extreme pressures (> 300 GPa) and the search for the nonmolecular metallic state.

Numerous experimental areas where continued progress is expected in the immediate future have been highlighted here. In particular, the use of synchrotron radiation is likely to reap important rewards. On the theoretical side, a number of uncertainties remain, including rather fundamental problems such as the need to treat the nuclear and electronic degrees of freedom on the same footing and going beyond the local-density approximation. The recently documented unexpected behavior of hydrogen at high pressure leads to the possibility of truly novel physics at ultrahigh pressures. Using the analogy to the discovery of superfluidity and superconductivity at extreme temperature conditions, such studies may lead to novel physical phenomena unique to extreme pressures. Meanwhile, the developments outlined here continue to demonstrate the power of the pressure variable for deepening our understanding of condensed matter.

ACKNOWLEDGMENTS

REFERENCES

Abrikosov, A. A., 1954, Astron. Zh. **31**, 112.
Anderson, P. W., 1958, Phys. Rev. **109**, 1492.
Ashcroft, N. W., 1968, Phys. Rev. Lett. **21**, 1748.
Ashcroft, N. W., 1990, Phys. Rev. B **41**, 10963.
Ashcroft, N. W., 1991a, *Molecular Solids under High Pressure*, edited by R. Pucci and G. Piccitto (Elsevier, Amsterdam), p. 201.
Ashcroft, N. W., 1991b, *Frontiers of High-Pressure Research*, edited by H. D. Hochheimer and R. D. Etters (Plenum, New York), p. 115.
Ashcroft, N. W., 1993, J. Non-Cryst. Solids **156-158**, 621.
Balchan, A. S., and H. G. Drickamer, 1961, J. Chem. Phys. **34**, 1948.
Barbee, T. W., A. Garcia, and M. L. Cohen, 1989, Nature **340**, 369.
Barbee, T. W., A. Garcia, M. L. Cohen, and J. L. Martins, 1989, Phys. Rev. Lett. **62**, 1150.
Berkhout, P. J., and I. F. Silvera, 1979, J. Low Temp. Phys. **36**, 231.
Bozio, R., and C. Pecile, 1991, *Spectroscopy of Advanced Materials*, edited by R. J. H. Clark and R. E. Hester (Wiley, New York), p. 1.
Brovman, E. G., Y. Kagan, and A. Kholas, 1972, Zh. Eksp. Teor. Fiz. **62**, 1492 [Sov. Phys. JETP **35**, 783 (1972)].
Brown, D. M., and W. B. Daniels, 1992, Phys. Rev. A **45**, 6429.
Chacham, H., and S. G. Louie, 1991, Phys. Rev. Lett. **66**, 64.
Dion, P., and A. D. May, 1973, Can. J. Phys. **51**, 36.
Doran, M. B., and I. J. Zucker, 1971, J. Phys. C, Solid State Phys. **4**, 307.
Duffy, T. S., W. Vos, C. S. Zha, R. J. Hemley, and H. K. Mao, 1994, Science **263**, 1590.
Eggert, J. H., 1991, Ph.D. thesis (Harvard University).
Eggert, J. H., K. A. Goettel, and I. F. Silvera, 1990, Europhys. Lett. **11**, 775.
Eggert, J. H., R. J. Hemley, H. K. Mao, and J. L. Feldman, 1994, in *High-Pressure Science and Technology*, edited by S. C. Schmidt, J. W. Shaner, G. A. Samara, and M. Ross (AIP, New York), in press.
Eggert, J. H., H. K. Mao, and R. J. Hemley, 1993, Phys. Rev. Lett. **70**, 2301.
Eggert, J. H., H. K. Mao, and R. J. Hemley, 1994, J. Lumin. (in press).
Eggert, J. H., F. Moshary, W. J. Evans, H. E. Lorenzana, K. A. Goettel, I. F. Silvera, and W. C. Moss, 1991, Phys. Rev. Lett. **66**, 193.
Eggert, J. H., C. S. Zha, R. J. Hemley, and H. K. Mao, 1992, J. Low. Temp. Phys. **89**, 707.
Feldman, J. L., J. de Kinder, J. H. Eggert, R. J. Hemley, and H. K. Mao, 1994, Bull. Am. Phys. Soc. **39**, 336.
Fowler, R. H., 1926, Mon. Not. R. Astron. Soc. **87**, 114.
Friedli, C., and N. W. Ashcroft, 1977, Phys. Rev. B **16**, 662.
Garcia, A., T. W. Barbee, M. L. Cohen, and I. F. Silvera, 1990, Europhys. Lett. **13**, 355.
Garcia, A., M. L. Cohen, J. H. Eggert, F. Moshary, W. J. Evans, K. A. Goettel, and I. F. Silvera, 1992, Phys. Rev. B **45**, 9709.
Ginzburg, V., 1978, *Key Problems in Physics and Astrophysics* (Mir, Moscow).
Glazkov, V. P., S. P. Besedin, I. N. Goncharenko, A. V. Irodova, I. N. Makarenko, V. A. Somenkov, S. M. Stishov, and S. S. Shilsteyn, 1988, Pis'ma Zh. Eksp. Teor. Fiz. **47**, 569 [JETP Lett. **47**, 661 (1988)].

Hanfland, M., A. Brillante, A. Girlando, and K. Syassen, 1988, Phys. Rev. B 38, 1456.

Hanfland, M., R. J. Hemley, and H. K. Mao, 1991, Phys. Rev. B 43, 8767.

Hanfland, M., R. J. Hemley, and H. K. Mao, 1993, Phys. Rev. Lett. 70, 3760.

Hanfland, M., R. J. Hemley, and H. K. Mao, 1994, in *High-Pressure Science and Technology*, edited by S. C. Schmidt, J. W. Shaner, G. A. Samara, and M. Ross (AIP, New York), in press.

Hanfland, M., R. J. Hemley, H. K. Mao, and G. P. Williams, 1992, Phys. Rev. Lett. 69, 1129.

Hemley, R. J., J. H. Eggert, and H. K. Mao, 1993, Phys. Rev. B 48, 5779.

Hemley, R. J., A. F. Goncharov, J. H. Eggert, M. Hanfland, and H. K. Mao, 1994, unpublished.

Hemley, R. J., M. Hanfland, and H. K. Mao, 1991, Nature 350, 488.

Hemley, R. J., and H. K. Mao, 1988, Phys. Rev. Lett. 61, 857.

Hemley, R. J., and H. K. Mao, 1989, Phys. Rev. Lett. 63, 1393.

Hemley, R. J., and H. K. Mao, 1990, Science 249, 391.

Hemley, R. J., and H. K. Mao, 1992, Phys. Lett. A 163, 429.

Hemley, R. J., H. K. Mao, L. W. Finger, A. P. Jephcoat, R. M. Hazen, and C. S. Zha, 1990, Phys. Rev. B 42, 6458.

Hemley, R. J., H. K. Mao, M. Hanfland, J. H. Eggert, C. S. Zha, and J. F. Shu, 1993, in *Strongly Coupled Plasma Physics*, edited by H. M. Van Horn and S. Ichimaru (University of Rochester Press, Rochester, N.Y.), p. 3.

Hemley, R. J., H. K. Mao, and J. F. Shu, 1990, Phys. Rev. Lett. 65, 2670.

Hemley, R. J., Z. G. Soos, M. Hanfland, and H. K. Mao, 1994, Nature, in press.

Hohl, D., V. Natoli, D. M. Ceperley, and R. M. Martin, 1993, Phys. Rev. Lett. 71, 541.

Hu, J., H. K. Mao, J. F. Shu, and R. J. Hemley, 1994, in *High-Pressure Science and Technology*, edited by S. C. Schmidt, J. W. Shaner, G. A. Samara, and M. Ross (AIP, New York), in press.

Huber, K. P., and G. Herzberg, 1979, *Molecular Spectra and Molecular Structure, IV* (Van Nostrand, N.Y.).

Jayaraman, A., 1983, Rev. Mod. Phys. 55, 65.

Kaxiras, E., J. Broughton, and R. J. Hemley, 1991, Phys. Rev. Lett. 67, 1138.

Kimball, J. C., C. Y. Fong, and Y. R. Shen, 1981, Phys. Rev. B 23, 4946.

Landau, L., 1935, Phys. Z. Sowjetunion 8, 113.

Lee, S.-H., M. S. Conradi, and R. E. Norberg, 1989, Phys. Rev. B 40, 12492.

Li, M., M. Hanfland, R. J. Hemley, and H. K. Mao, 1994, Bull. Am. Phys. Soc. 39, 336.

Lorenzana, H. E., I. F. Silvera, and K. A. Goettel, 1989, Phys. Rev. Lett. 63, 2080.

Lorenzana, H. E., I. F. Silvera, and K. A. Goettel, 1990, Phys. Rev. Lett. 64, 1939.

Loubeyre, P., R. LeToullec, and J. P. Pinceaux, 1992, Phys. Rev. B 45, 12844.

Maggs, A. C., and N. W. Ashcroft, 1987, Phys. Rev. B 36, 7586.

Mao, H. K., 1989, in *Molecular Systems at Very High Density*, edited by A. Polian, P. Loubeyre, and N. Boccara (Plenum, New York), p. 221.

Mao, H. K., and P. M. Bell, 1976, Carnegie Inst. Washington Yearb. 75, 827.

Mao, H. K., and P. M. Bell, 1977, Carnegie Inst. Washington Yearb. 77, 904.

Mao, H. K., and P. M. Bell, 1979, Science 203, 1004.

Mao, H. K., and P. M. Bell, 1981, Rev. Sci. Instrum. 52, 615.

Mao, H. K., P. M. Bell, and R. J. Hemley, 1985, Phys. Rev. Lett. 55, 99.

Mao, H. K., and R. J. Hemley, 1989, Science 244, 1462.

Mao, H. K., and R. J. Hemley, 1991, Nature 351, 721.

Mao, H. K., R. J. Hemley, and M. Hanfland, 1990, Phys. Rev. Lett. 65, 484.

Mao, H. K., R. J. Hemley, and M. Hanfland, 1992, Phys. Rev. B 45, 8108.

Mao, H. K., A. P. Jephcoat, R. J. Hemley, L. W. Finger, C. S. Zha, R. M. Hazen, and D. E. Cox, 1988, Science 239, 1131.

Mao, H. K., J. Xu, and P. M. Bell, 1984, in *High Pressure in Science and Technology*, edited by C. Homan, R. K. MacCrone, and E. Whalley (North-Holland, New York), p. 327.

Matveev, V. V., I. V. Medvedeva, V. V. Prut, P. A. Suslov, and S. A. Shibaev, 1984, Pis'ma Zh. Eksp. Teor. Fiz. 39, 219 [JETP Lett. 39, 261 (1984)].

Mills, R. L., D. H. Leibenberg, J. C. Bronson, and L. C. Schmidt, 1980, Rev. Sci. Instrum. 51, 891.

Mott, N., 1990, *Metal-Insulator Transitions,* 2nd Edition (Taylor & Francis, London).

Moulopoulos, K., and N. W. Ashcroft, 1991, Phys. Rev. Lett. 66, 2915.

Nagara, H., and T. Nakamura, 1992, Phys. Rev. Lett. 68, 2468.

Natoli, V., R. M. Martin, and D. M. Ceperley, 1993, Phys. Rev. Lett. 70, 1952.

Nellis, W. J., A. C. Mitchell, P. C. McCandless, D. J. Erskine, and S. T. Weir, 1992, Phys. Rev. Lett. 68, 2937.

Nellis, W. J., A. C. Mitchell, M. V. Thiel, G. J. Devine, and R. J. Trainor, 1983, J. Chem. Phys. 79, 1480.

Oliva, J., and N. W. Ashcroft, 1981, Phys. Rev. B 23, 6399.

Ramaker, D. E., L. Kumar, and F. E. Harris, 1975, Phys. Rev. Lett. 34, 812.

Ross, M., F. R. Ree, and D. A. Young, 1983, J. Chem. Phys. Lett. 79, 1487.

Ruoff, A. L., and C. A. Vanderborgh, 1991, Phys. Rev. Lett. 66, 754; 1993, 71, 4279(E).

Schuch, A. F., R. L. Mills, and D. A. Depatie, 1967, Phys. Rev. 165, 1032.

Sharma, S. K., H. K. Mao, and P. M. Bell, 1980a, Phys. Rev. Lett. 44, 886.

Sharma, S. K., H. K. Mao, and P. M. Bell, 1980b, in *High Pressure Science and Technology*, edited by B. Vodar and P. Marteau (Pergamon, Oxford), p. 1101.

Shimizu, H., E. M. Brody, H. K. Mao, and P. M. Bell, 1981, Phys. Rev. Lett. 47, 128.

Silvera, I. F., 1980, Rev. Mod. Phys. 52, 393.

Silvera, I. F., 1989, in *Simple Molecular Systems at Very High Density,* edited by A. Polian, P. Loubeyre, and N. Bocarra (Plenum, New York), p. 33.

Silvera, I. F., and V. V. Goldman, 1978, J. Chem. Phys. 69, 4209.

Silvera, I. F., S. J. Jeon, and H. E. Lorenzana, 1992, Phys. Rev. B 46, 5791.

Silvera, I. F., and R. J. Wijngaarden, 1981, Phys. Rev. Lett. 47, 39.

Sullivan, N. S., M. Devoret, B. P. Cowan, and C. Urbina, 1978, Phys. Rev. B 17, 5016.

Surh, M. P., T. W. Barbee, and C. Mailhiot, 1993, Phys. Rev. Lett. 70, 4090.

van Kranendonk, J., 1983, *Solid Hydrogen* (Plenum, New York).

van Straaten, J., and I. F. Silvera, 1988a, Phys. Rev. B 37, 1989.

van Straaten, J., and I. F. Silvera, 1988b, Phys. Rev. B **37**, 6478.

Wigner, E., and H. B. Huntington, 1935, J. Chem. Phys. **3**, 764.

Wijngaarden, R. J., V. V. Goldman, and I. F. Silvera, 1983, Phys. Rev. B **27**, 5084.

Wijngaarden, R. J., A. Lagendijk, and I. F. Silvera, 1982, Phys. Rev. B **26**, 4957.

Zha, C. S., T. S. Duffy, H. K. Mao, and R. J. Hemley, 1993, Phys. Rev. B **48**, 9246.